ILLINOIS CENTER FOR TRANSPORTATION

CIVIL ENGINEERING STUDIES
Illinois Center for Transportation Series No. 21-019
UILU-ENG-2021-2019
ISSN: 0197-9191

Evaluation of Electrochemical Treatment for Removal of Arsenic and Manganese from Field Soil

Prepared By
Taiwo Akinleye
Idil Deniz Akin
Amanda Hohner
Indranil Chowdhury
Richards Watts
Xianming Shi
Washington State University
Brendan Dutmer
Highland Community College
James Mueller
Will Moody
Provectus Environmental Products, Inc.

Research Report No. FHWA-ICT-21-014

The fourth of four reports of the findings of

ICT PROJECT R27-183-HS
Evaluation of On-Site and In situ Treatment Alternatives for Contaminated Soils

https://doi.org/10.36501/0197-9191/21-019

Illinois Center for Transportation

June 2021

TECHNICAL REPORT DOCUMENTATION PAGE

1. Report No.	2. Government Accession No.	3. Recipient's Catalog No.
FHWA-ICT-21-014	N/A	N/A

4. Title and Subtitle	5. Report Date
Evaluation of Electrochemical Treatment for Removal of Arsenic and Manganese from Field Soil	June 2021
	6. Performing Organization Code N/A

7. Authors	8. Performing Organization Report No.
Taiwo Akinleye, Idil Deniz Akin (https://orcid.org/0000-0002-1946-4951), Amanda Hohner (https://orcid.org/0000-0001-7704-4464), Indranil Chowdhury, Richards J. Watt, Xianming Shi (https://orcid.org/0000-0003-3576-8952), Brendan Dutmer, Jim Mueller, and Will Moody	ICT-21-019 UILU-2021-2019

9. Performing Organization Name and Address	10. Work Unit No.
Illinois Center for Transportation Department of Civil and Environmental Engineering University of Illinois at Urbana-Champaign 205 North Mathews Avenue, MC-250 Urbana, IL 61801	N/A
	11. Contract or Grant No. R27-183-HS

12. Sponsoring Agency Name and Address	13. Type of Report and Period Covered
Illinois Department of Transportation (SPR) Bureau of Research 126 East Ash Street Springfield, IL 62704	Final Report 2/1/18–6/30/21
	14. Sponsoring Agency Code

15. Supplementary Notes

Conducted in cooperation with the U.S. Department of Transportation, Federal Highway Administration.

https://doi.org/10.36501/0197-9191/21-019

16. Abstract

Soils containing inorganic compounds are frequently encountered by transportation agencies during construction within the right-of-way, and they pose a threat to human health and the environment. As a result, construction activities may experience project delays and increased costs associated with management of inorganic compounds containing soils required to meet environmental regulations. Recalcitrance of metal-contaminated soils toward conventional treatment technologies is exacerbated in clay or organic content-rich fine-grained soils with low permeability and high sorption capacity because of increased treatment complexity, cost, and duration. The objective of this study was to develop an accelerated in situ electrochemical treatment approach to extract inorganic compounds from fine-grained soils, with the treatment time comparable to excavation and off-site disposal. Three reactor experiments were conducted on samples collected from two borehole locations from a field site in Illinois that contained arsenic (As)(~7.4 mg/kg) and manganese (Mn)(~700 mg/kg). A combination of hydrogen peroxide (H_2O_2) and/or citrate buffer solution was used to treat the soils. A low-intensity electrical field was applied to soil samples using a bench-scale reactor that resembles field-scale in situ electrochemical systems. For the treatment using 10% H_2O_2 and citrate buffer solution, average removal of 23% and 8% were achieved for Mn and As, respectively. With 4% H_2O_2 and citrate buffer, 39% and 24% removal were achieved for Mn and As; while using only citrate buffer as the electrolyte, 49% and 9% removal were achieved for Mn and As, respectively. All chemical regimes adopted in this study reduced the inorganic compound concentrations to below the maximum allowable concentration for Illinois as specified by the Illinois Environmental Protection Agency. The results from this work indicate that electrochemical systems that leverage low concentrations of hydrogen peroxide and citrate buffer can be effective for remediating soils containing manganese and arsenic.

17. Key Words	18. Distribution Statement
Electrochemical Treatment, Contaminant, Sorption, Permeability	No restrictions. This document is available through the National Technical Information Service, Springfield, VA 22161.

19. Security Classif. (of this report)	20. Security Classif. (of this page)	21. No. of Pages	22. Price
Unclassified	Unclassified	41 + appendices	N/A

ACKNOWLEDGMENT, DISCLAIMER, MANUFACTURERS' NAMES

This publication is based on the results of **ICT-R27-183-HS: Evaluation of On-Site and In situ Treatment Alternatives for Contaminated Soils**. ICT-R27-183-HS was conducted in cooperation with the Illinois Center for Transportation; the Illinois Department of Transportation; and the U.S. Department of Transportation, Federal Highway Administration.

Members of the Technical Review Panel (TRP) were the following:

- Doug Dirks—TRP Co-chair, Illinois Department of Transportation
- Jim Curtis—TRP Co-chair, Illinois Department of Transportation
- Doug Liniger—Illinois Department of Transportation
- Greg Dunn—Illinois Environmental Protection Agency
- Viraj Perera—Illinois Department of Transportation
- Tyler Petersen—Illinois Department of Transportation
- Kyle Rominger—Illinois Environmental Protection Agency
- Bart Sherer—Illinois Department of Transportation
- JD Stevenson—Federal Highway Administration
- Heather Shoup—Illinois Department of Transportation
- Megan Swanson- Illinois Department of Transportation
- Dan Wakefield—Illinois Department of Transportation
- Andrew Anderson—Illinois State Geological Survey

The contents of this report reflect the view of the authors, who are responsible for the facts and the accuracy of the data presented herein. The contents do not necessarily reflect the official views or policies of the Illinois Center for Transportation, the Illinois Department of Transportation, or the Federal Highway Administration. This report does not constitute a standard, specification, or regulation.

Trademark or manufacturers' names appear in this report only because they are considered essential to the object of this document and do not constitute an endorsement of product by the Federal Highway Administration, the Illinois Department of Transportation, or the Illinois Center for Transportation.

The work presented in this report was previously published in 2021 by Washington State University in Taiwo Akinleye's master's thesis (Akinleye, 2021). In many instances, tables, figures, and text presented within this report were taken from the student's thesis (Akinleye, 2021), unless otherwise indicated.

EXECUTIVE SUMMARY

Soils that contain inorganic compounds are frequently encountered by transportation agencies during construction within the right-of-way, and they pose a threat to human health and the environment. As a result, construction activities may experience project delays and increased costs associated with management of inorganic compounds containing soils required to meet environmental regulations. Treatment alternatives such as chemical oxidation, air stripping, thermal desorption, and biological treatment often require contaminants to be in the aqueous phase, where contaminants have increased contact with the treatment solution. However, recalcitrance of metal-contaminated soils toward conventional treatment technologies is exacerbated in clay or organic content-rich fine-grained soils with low permeability and high sorption capacity because of increased treatment complexity, cost, and duration.

The objective of this study was to develop an accelerated in situ electrochemical treatment approach to extract inorganic compounds from fine-grained soils, with the treatment time comparable to excavation and off-site disposal. Three bench-scale reactor experiments were conducted on samples collected from two borehole locations from a field site in Illinois containing arsenic (As)(~7.4 mg/kg) and manganese (Mn)(~700 mg/kg). A combination of hydrogen peroxide (H_2O_2) or citrate buffer solution was used to treat the soils. A low-intensity electrical field was applied to soil samples using a bench-scale reactor that resembles field-scale in situ electrochemical (EC) systems. For the treatment using 10% H_2O_2 and citrate buffer solution, average contaminant removal of 23% and 8% were achieved for Mn and As, respectively. With 4% H_2O_2 and citrate buffer, 39% and 24% contaminant removal were achieved for Mn and As; while using only citrate buffer as the electrolyte, 49% and 9% contaminant removal were achieved for Mn and As, respectively. All chemical regimes adopted in this study reduced the contaminant concentrations to below the maximum allowable concentration for Illinois as specified by the Illinois Environmental Protection Agency. The results from this work indicate that EC systems that leverage low concentrations of hydrogen peroxide and citrate buffer can be effective for remediating soils containing manganese and arsenic.

TABLE OF CONTENTS

CHAPTER 1: INTRODUCTION 1

REACTOR EXPERIMENT USING PROTOTYPE SOIL 2

STUDY SITE AND FIELD SOIL SAMPLING 2

Scope 2

Equipment 3

Procedures 3

CHAPTER 2: SOIL CHARACTERISTICS 4

CHAPTER 3: LABORATORY EXPERIMENTS 6

STANDARD TECHNIQUES AND METHODS 6

In Situ Moisture Content 6

Soil pH 6

Soil Plasticity 6

Grain Size Distribution 6

Unconfined Compressive Strength 6

Metal Analysis 6

PRETREATMENT EXPERIMENTS 7

REACTOR EXPERIMENTS 7

Experimental Setup 7

Working Principle 9

Reactor Loading 9

Chemical Reagent Selection and Application 9

Electrochemical Treatment Sequence 10

Reactor Performance Checks: Daily Measurements 10

Post-treatment Experiments 11

CHAPTER 4: RESULTS AND DISCUSSION 12

FIRST REACTOR RUN 12

Pretreatment 12

Post-treatment 12

SECOND REACTOR RUN **19**
Pretreatment 19
Post-treatment 20
THIRD REACTOR RUN **26**
Pretreatment 26
Post-treatment 27

CHAPTER 5: RESEARCH SUMMARY, CONCLUSIONS, RECOMMENDATIONS, BENEFITS, AND COSTS **34**
RESEARCH SUMMARY **34**
CONCLUSIONS **34**
TREATMENT RECOMMENDATIONS **35**
RECOMMENDATIONS FOR FIELD IMPLEMENTATION **35**
BENEFITS OF ELECTROCHEMICAL TREATMENT **36**
ESTIMATE OF FIELD-SCALE ELECTROCHEMICAL TREATMENT COSTS **36**

REFERENCES **38**

APPENDIX A: FIELD SAMPLING **42**

APPENDIX B: LABORATORY TEST DATA **46**

LIST OF FIGURES

Figure 1. Graph. Particle size distribution of the field soil (R = reactor run). 5

Figure 2. Photo. Bench-scale electrochemical reactor: (A) HDPE soil reactor, (B) surcharge plate, (C) anode electrode, (D) auxiliary electrode, (E) cathode electrode, (F) glass fiber filter paper, (G) reservoir, (H) direct current power supply, (I) electric cables, (J) tygon tube, (K) cathode-well overflow tank, (L) peristaltic pump, and (M) anode-well overflow tank. 8

Figure 3. Graph. pH measurement at electrode wells (R1). 13

Figure 4. Equation. Electrolysis of water at anode and cathode wells..... 13

Figure 5. Graph. pH distribution of soil per layer post reactor run (R1). The numbers shown for each sample point indicate the change in pH from the initial conditions (Δ pH). 14

Figure 6. Graph. Daily measured current across the reactor cell (R1). 15

Figure 7. Graph. Moisture content distribution in soil post-treatment (R1). The numbers shown for each sample point indicate the final MC normalized by the initial MC (MC/MC_0)..... 16

Figure 8. Graph. Inorganic compound concentration post reactor run (R1): (A) As and (B) Mn. 17

Figure 9. Graph. Soil plasticity pre- and post-treatment (R1). Pretreatment refers to the untreated field soil and post-treatment refers to layers 1–4 (treated)..... 18

Figure 10. Graph. Soil plasticity vs unconfined compressive strength (R1). 19

Figure 11. Graph. Daily measured pH in anode, cathode, and cathode overflow wells (R2)..... 20

Figure 12. Graph. pH across soil matrix post-treatment (R2). The numbers shown for each sample point indicate the change in pH from the initial conditions (Δ pH). 21

Figure 13. Graph. Daily measured current across electrodes (R2). 22

Figure 14. Graph. Moisture content distribution in soil post-treatment (R2). The numbers shown for each sample point indicate the final MC normalized by the initial MC (MC/MC_0)..... 23

Figure 15. Graph. Contaminant concentration post reactor run (R2): (A) As and (B) Mn. 24

Figure 16. Graph. Soil plasticity pre- and post-treatment (R2). Pretreatment refers to the untreated field soil and post-treatment is layers 1–4 (treated)..... 25

Figure 17. Graph. Soil plasticity vs unconfined compressive strength (R2). 26

Figure 18. Graph. Daily measured pH in anode, cathode, and cathode overflow wells (R3)..... 27

Figure 19. Graph. pH across soil matrix post-treatment (R3). The numbers shown for each sample point indicate the change in pH from the initial conditions (Δ pH). 28

Figure 20. Graph. Daily measured current across electrodes (R3). 29

Figure 21. Graph. Moisture content distribution in soil post-treatment (R3). The numbers shown for each sample point indicate the final MC normalized by the initial MC (MC/MC_0)..... 30

Figure 22. Graph. Contaminant concentration post reactor run (R3): (A) As and (B) Mn. 31

Figure 23. Graph. Soil plasticity pre- and post-treatment (R3). Pretreatment refers to the untreated field soil and post treatment is layers 1–4 (treated). 32

Figure 24. Graph. Soil plasticity vs unconfined compressive strength (R3). 33

Figure 25. Photo. Field soil boring location..... 42

Figure 26. Photos. Rock Falls sample collection borings for B14 soil (Yard 244 @ 1004 E. Rock Falls Road / Rt 30, Rock Falls, Illinois)..... 43

Figure 27. Photos. Rock Falls sample collection borings for the B10 soil (Yard 244 @ 1004 E. Rock Falls Road / Rt 30, Rock Falls, Illinois)..... 44

Figure 28. Photo. Soil profile with depth at boring location..... 45

LIST OF TABLES

Table 1. Typical Index Properties of Sample Collection Site 4

Table 2. Summary of Electrochemical Regime by Experiment 10

Table 3. Approximate Cost for Treating 250 Cubic Yards (191 m^3) of Soil Co-contaminated with Organic and Inorganic Compounds 37

Table 4. Cost Summary for Electrochemical Treatment 37

Table 5. Particle Size Distribution 46

Table 6. Atterberg Limit Test for Sample 244-B10 (R1) 47

Table 7. Atterberg Limit Test for Sample 244-B14 (R2) 47

Table 8. Atterberg Limit Test for Sample 244-B14 (R3) 48

Table 9. Daily Measurement for First Reactor Experiment 49

Table 10. Daily Measurement for Second Reactor Experiment 51

Table 11. Daily Measurement for Third Reactor Experiment 52

LIST OF ACRONYMS AND ABBREVIATIONS

As: Arsenic
CHP: Catalyzed Hydrogen Peroxide
DOT: Department of Transportation
EO: Electro-osmosis
EC: Electrochemical
EM: Electromigration
EP: Electrophoresis
GPS: Global Positioning System
HDPE: High-Density Polyethylene
IAC: Illinois Administrative Code
ICT: Illinois Center for Transportation
ICPMS: Inductively coupled plasma mass spectrometry
IDOT: Illinois Department of Transportation
IEPA: Illinois Environmental Protection Agency
KED: kinetic energy discrimination
MAC: Maximum Allowable Concentration
MC: Moisture Content
MSA: Metropolitan Statistical Area
Mn: Manganese
Nan: Not a number
OM: Organic Matter
ROS: Reactive Oxygen Species
SHP: Stabilized Hydrogen Peroxide
UCS: Unconfined Compressive Strength
USCS: Unified Soil Classification System
USDA: United Stated Department of Agriculture
USEPA: United States Environmental Protection Agency

CHAPTER 1: INTRODUCTION

In recent years, construction on surface and in subsurface soils has experienced significant increases in cost and delay in construction time and approval of regulatory requirements for construction in the state of Illinois (ICT, 2018). One factor contributing to this is the need to satisfy environmental regulations associated with toxic/nontoxic organic and inorganic compounds in soils. Soil contamination results from human activities such as operation of industrial machineries, improper waste disposal, accidental spill and leakage from underground tanks or pipes conveying petroleum products, leachates from landfills, and waste from mining operations (Diamond & Hodge, 2007). These contaminants are commonly encountered during construction projects (ICT, 2018).

The need for timely and cost-effective treatment of contaminated soils has led to the development of several in situ treatment alternatives, including chemical oxidation, air stripping, thermal desorption, and biological treatment (e.g., Alcántara et al., 2008; Ammami et al., 2015). These treatment methods often require contaminants to be in the aqueous phase, where contaminants have increased contact with the treatment solution. However, fine-grained soils (i.e., silt and clay) are often characterized by low permeability (in the order of 10^{-6}–10^{-9} m/s); hence, migration of treatment solution into the soil matrix becomes challenging (Reddy & Cameselle, 2009). In addition, the large specific surface area and presence of soil organic matter (OM) fraction in fine-grained soils provide excellent sorption surface for metal contaminants (Duan et al., 2015; Patnaik, 2007), further hindering their removal.

Among several compounds often encountered in construction projects in Illinois, inorganic compounds rank amid the highest and are found to coexist in several regions (ICT, 2018). For example, the Illinois Center for Transportation (ICT) in 2018 reported arsenic (As) and manganese (Mn) as part of the major inorganic compounds exceeding their maximum allowable concentration (MAC) in soils as specified by the Illinois Administrative Code (35 IAC §1100 §§F, 2012). The fate of inorganic compounds in the subsurface, which includes their physical transport, chemical transformation, and retardation, is important to understanding the right treatment technique to employ (Reddy & Cameselle, 2009). Also, their transformation in the subsurface is influenced by several environmental conditions and soil properties, including pH, redox potential, cation exchange capacity of the solid matrix, presence of other metallic ions (including competition between them), soil composition, and concentration of the compound in the soil pore fluid (Merian et al., 2004).

Electrochemical treatment poses to address the wide range of environmental conditions and soil properties and therefore is an attractive alternative for the extraction of inorganic compounds from soil (e.g., Reddy & Cameselle, 2009). Over the years, electrochemical techniques have been used in solving a variety of soil stabilization and foundation engineering problems (Reddy & Cameselle, 2009; Zhang et al., 2017a, 2017b). This concept has also been of interest to geotechnical engineers as a technique for improving stability of excavations (Chappell & Burton, 1975), increasing pile strength (Butterfield & Johnson, 1980), stabilizing fine-grained soils (Mitchell & Wan, 1977), decreasing pile penetration resistance (Esrig, 1978), determining volume change and consolidation characteristics of soils (Jeyakanthan et al., 2011), as well as separating and filtrating materials in soils and solutions (Yukawa et al., 1976). In recent years, electrochemical techniques have been extended for

geoenvironmental engineering applications for the removal of various organic and inorganic contaminants from soils, sediments, sludge, and other solid porous matrices (Reddy & Cameselle, 2009). The use of electrochemical techniques to remediate inorganic compounds in soils has also been investigated under various experimental conditions (e.g., Pamukcu & Wittle, 1994; Kim & Kim, 2001; Ottosen et al., 2001). Studies on the mobilization of inorganic compounds in fine-grained soils (Acar et al., 1990; Yuan & Chiang, 2008) and transformation (Patnaik, 2007) have also been reported. Inorganic contaminant removal has been demonstrated by a combination of electrochemical and other techniques, including biotreatment in soils (Zhang et al., 2020). The application of electrokinetics and chemical augmentation in removing inorganic compounds have also been established for treatment of inorganic contaminants from mine tailings and artificially contaminated soils (Isosaari & Sillanpää, 2012).

Although existing studies on electrochemical treatment showed successful results, the technique can be improved for more efficient removal of various organic and inorganic contaminants in soils, sediments, sludge, and other solid porous matrices. One of the main challenges is scaling up the laboratory experiments to the field scale. Hence, this study aims to develop an electrochemical technique to remediate clayey soils that contain inorganic compounds (As and Mn). The developed technique is scalable to the field and treats the contaminated soils within a short time frame, equivalent to the time and cost of excavation and off-site disposal. The remainder of the report will use the terms “inorganic compounds” and “inorganic contaminants” interchangeably to refer to As and Mn, respectively.

REACTOR EXPERIMENT USING PROTOTYPE SOIL

A laboratory study was conducted using kaolinite clay artificially spiked with model inorganic compounds (chromium and manganese), as described in the Task 3 report (Pelletier et al., 2021). This was done to understand the behavior of the model soil with an electrochemical process as well as to optimize the mechanisms required for effective extraction of the inorganic compounds of concern. The chemical regime used for the fifth and sixth experiments (kaolinite soil) in the Task 3 report (Pelletier et al., 2021) showed promising effectiveness in remediating co-contaminated Illinois soil, forming the basis for adopting this method for the reactor run treatment of the field soil. Changes made to the field soil experiment, except otherwise stated, include pH adjustment carried out twice daily (every 12 hours) to better regulate the pH at both electrode wells. In addition, pH conditioning reagents were prepared in a solution form, instead of powder, in the preliminary study. The changes to the method are described in more detail in Chapter 3 of this report.

STUDY SITE AND FIELD SOIL SAMPLING

Scope

Representative subsurface soil samples were collected from two Illinois locations at the Rock Falls site (Yard 244 @ 1004 E. Rock Falls Rd / Rt 30, Rocks Falls, IL) on July 24, 2019. Two 5 US gallon buckets of soil were collected from area 244-B10 and two 5 US gallon buckets of soil were collected from area 244-B14 (Appendix A) for a total of four 5 US gallon buckets. Soil sampling depths were limited to that which can be reached without the use of a drill rig, direct push, or other mechanized equipment. The

concentrations of inorganic compounds of concern are such that Level D personal protective equipment (PPE) was required as detailed below.

Equipment

Provectus Environmental Products (Consultant)

- Maps / plot plan
- Safety equipment, per Level D PPE (reflective vest, steel toe boots, gloves)
- Camera
- Four 5 US gallon plastic buckets with screw-top lids
- Spade
- Post-hole auger
- Hand auger
- Rake
- Twenty-five US gallons of clean topsoil
- Grass seed

Fehr-Graham (Subcontractor)

- Safety equipment, per Level D PPE (reflective vest, steel toe boots, gloves)
- Tape measure
- Traffic cones, stakes, or flags
- Logbook
- Sample labels, clear shipping tape, duct tape
- Chain of Custody records and custody seals
- Field data sheets and sample labels
- Decontamination supplies / equipment
- Canvas or plastic sheeting

Procedures

Sample Collection

The upper 1 ft of surface soil was removed manually with a shovel from an area measuring approximately 2 ft × 2 ft, and soil samples were collected manually at a depth of 1 ft to approximately 5 ft beneath the soil surface using a post-hole digger or hand auger. The samples were then placed in the labelled bucket(s) and the lids were secured tightly and shipped to the laboratory. Global positioning system (GPS) coordinates were recorded for each sample location within the nearest 50 ft (Appendix A). Soils in different buckets were not mixed prior to the experiment, as they were obtained from different borehole locations and the depth of collection for each bucket was not specified.

CHAPTER 2: SOIL CHARACTERISTICS

One common soil type encountered in Illinois is known as the Drummer soil series, which are defined as “very deep, poorly drained soils formed in loess or other silty material and in the underlying loamy stratified outwash on nearly level or depressional parts of outwash plains, stream terraces, and till plains” (USDA, 2015, p. 1). The typical Drummer soil series spans the uppermost 5 ft of the surface and is composed primarily of silty clay loam. Clay, silt, and sand are fine soil particles whose diameters are less than 0.002 mm, between 0.002 mm and 0.05 mm, and between 0.05 mm and 2.0 mm, respectively (Adewunmi, 2019). On average, Drummer soils consist of 20%–35% clay, with less than 15% sand content, and are majorly composed of fine-grained silts (USDA, 2015, p. 1). Furthermore, the Drummer soil series is rich in natural OM content at the surface and contains a high presence of oxidized iron and manganese masses below. Table 1 summarizes typical index properties of a sample collection site (USEPA, 2001).

Table 1. Typical Index Properties of Sample Collection Site

Bulk Density	1.76 g/cm^3 (110 lb./ft^3)
Void Ratio	0.43
Porosity	0.75
Specific Gravity	2.65

Soil samples collected from the field show characteristics of Drummer soils and were classified according to the Unified Soil Classification System (USCS) (ASTM D2487) as inorganic clay of low plasticity (CL). Figure 1 presents the particle size distribution of the study soils obtained from the combined sieve (ASTM D6913) and hydrometer (ASTM D7928) analysis. R1 (B-10), R2 (B-14), and R3 (B-14) designations imply the first, second, and third reactor experiment, respectively. B-10 and B-14 are the borehole designations where the samples were obtained.

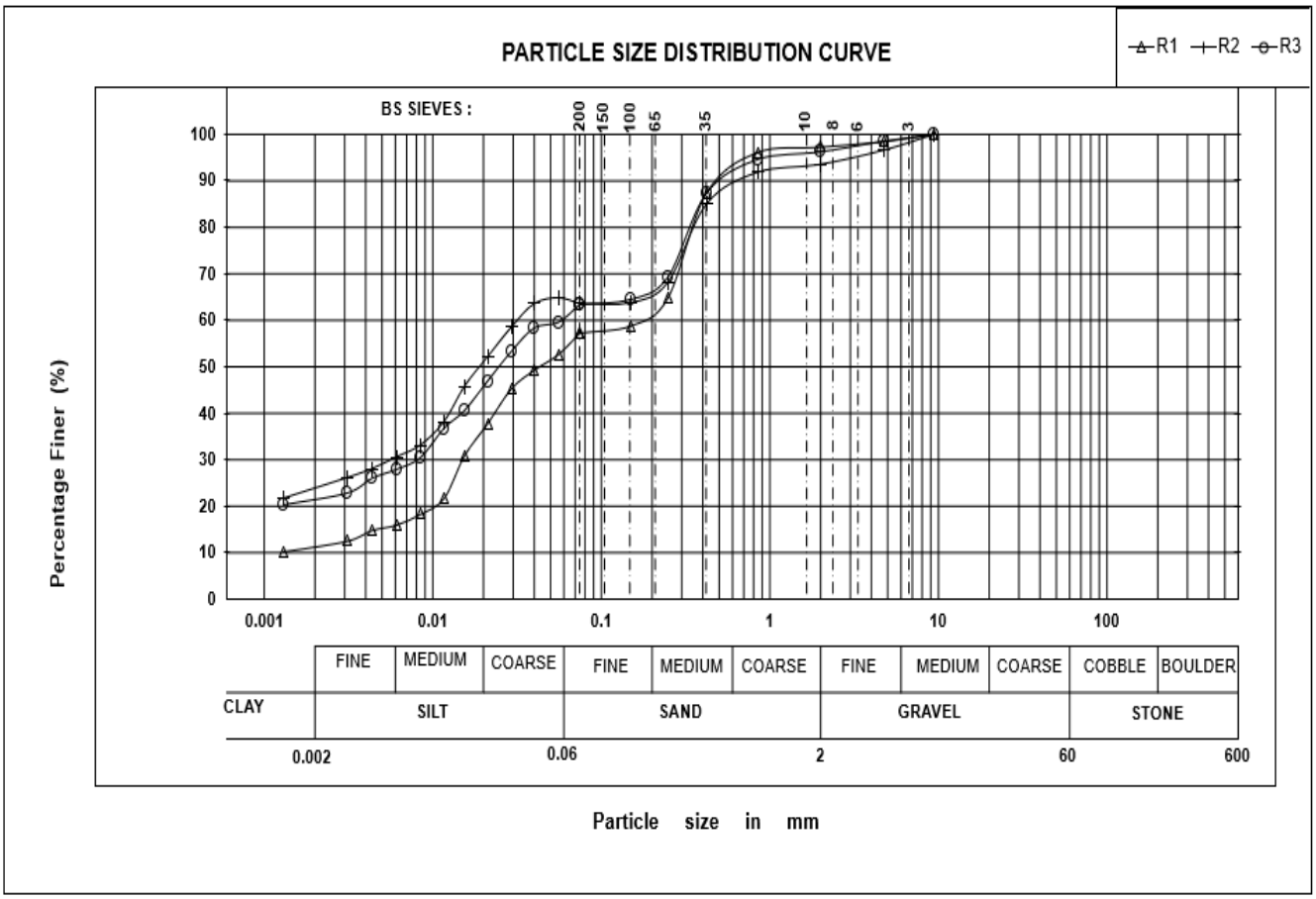

Figure 1. Graph. Particle size distribution of the field soil (R = reactor run).

CHAPTER 3: LABORATORY EXPERIMENTS

STANDARD TECHNIQUES AND METHODS

In Situ Moisture Content

Moisture content (MC) analysis of the soil was carried out in accordance with ASTM D2216-19. Samples were placed in an oven with an average temperature of 105°C for 24 hours, and the mass of the soil before and after oven drying was measured to calculate water content.

Soil pH

The average pH of the soil samples was measured using a VWR® Symphony™ B10P Benchtop Meter with a VWR® 89231-596 pH electrode and integrated temperature sensor. Ten grams of soil samples were added to 50 mL vial tubes, and 10 mL deionized water was added, vortexed, and allowed to equilibrate for 24 hours before measurement.

Soil Plasticity

Soil plasticity was measured in accordance with ASTM D4318-17, “Standard Test Methods for Liquid Limit (LL), Plastic Limit (PL), and Plasticity Index (PI) of Soils” (See Tables 6, 7, and 8 in Appendix B).

Grain Size Distribution

The grain size of a selected representative elementary volume of the soil was determined using the combined results from the sieve analysis, in accordance with ASTM D6913 for larger particles retained on the sieve No. 200, and the hydrometer test, in accordance with ASTM D7928 on fine content that was washed through sieve No. 200 (See Table 5 in Appendix B).

Unconfined Compressive Strength

Cylindrical specimens 3.3 cm in diameter and 7.1 cm in height were prepared using Harvard miniature compacting equipment. Specimens were prepared at a preselected water content (8%–15.7%) and void ratio (0.74). With known volume of the compaction mold, the required mass of soil and water was calculated and thoroughly hand mixed for approximately 3 minutes to obtain a homogenous mixture with no lumps formed. The soil-water mixture was compacted in the mold in three equal thickness layers. Twenty blows were applied with a 9 kg dynamic compaction hammer for each layer. The compacted specimens were carefully extruded and tested immediately to avoid loss of moisture. Unconfined compressive strength (UCS) testing was performed at a strain rate of 0.4%/min.

Metal Analysis

Metal concentration in soil was measured using a PerkinElmer NexION™ 350X Inductively Coupled Plasma Mass Spectrometry (ICPMS) in accordance with EPA Method 6020B: Inductively Coupled Plasma Mass Spectrometry for use with kinetic energy discrimination mode (KED; also known as collision mode) to minimize polyatomic interferences. The soil pore fluid was extracted following USEPA Method 3050B (SW-846): Acid Digestion of Sediments, Sludges, and Soils (USEPA, 2021). One gram of wet soil sample was distributed in 15 mL capped Hach vials and placed in aluminum reaction

blocks on a hot plate. The vials were heated at 95 ± 5°C for 30 to 60 minute intervals, following sequential additions of 6 mL of 35% nitric acid (HNO_3), 4 mL of 70% HNO_3, and 1 mL of 30% H_2O_2. A fourth heating period was applied to samples in which effervescence was still occurring, or brown gas was present, such that complete metal oxidation to water-soluble nitrate salts was achieved. Digested samples were vacuum filtered through 0.22 µm-pore diameter glass fiber filters and diluted with 1% HNO_3 to a 1000-fold (ug/L) dilution factor. Argon gas (99.985%) was used for plasma, auxiliary, and nebulizer gas flow. Ultrapure helium gas (>99.999% He) was used in the collision cell for KED. Samples were measured with 40 sweeps/reading, 1 reading/replicate, and 3 replicates. Quality control checks were performed at the beginning and end of each run, and after every tenth measurement, with 2 to 4 standard concentrations. Internal indium standards were added to each blank, standard, and sample. Sample cross-contamination was prevented by applying a 60 second wash cycle, 60 second sample flush, and 30 second read delay. The washing solution varied between 1% and 10% HNO_3, depending on concentrations present in the samples (i.e., highly contaminated samples required 10% acid to remove contamination from the ICPMS cones between runs, whereas highly diluted samples required only 1% acid to restore baseline). Samples were only analyzed after satisfying calibration with $R^2 > 0.99$ for the metal of concern.

PRETREATMENT EXPERIMENTS

Prior to loading the reactor, the field soil properties were evaluated to provide baseline information useful for application during the treatment process. To determine the necessary volume to be loaded into the reactor and to achieve the targeted void ratio, the moisture content of the field soil was measured. In addition, sieve analysis and the hydrometer test were carried out to obtain the particle size distribution of the field soil. This information may also provide an indirect inorganic compound concentration relationship via the percent of fine content present. The pH of the soils was measured to have an idea of the buffering capacity and required pH control during the experiment run. The soil plasticity using Atterberg limit tests was calculated for comparison with post-treatment soil to understand the influence of the treatment process on soil plasticity. The unconfined compression strength (UCS) test was also conducted for strength comparison post-treatment. The initial concentration of inorganic compounds of concern were analyzed to evaluate removal efficiency using the electrochemical method.

REACTOR EXPERIMENTS

Experimental Setup

Figure 2 presents the experimental setup and connections used for this study. The high-density polyethylene (HDPE) bench-scale reactor (N) designed and fabricated for the kaolinite soil experiment run, described in Pelletier et al. (2021), was modified and used for this study to remediate the field soil samples. The volume of the reactor is 8.5 L, and it is a prototype of field-scale in situ EC systems. Two prefabricated electrode wells (A) made from chlorinated polyvinyl chloride material were placed 20 cm apart on opposite corners of the reactor, and tygon tubes (J) were used for connection to the peristaltic pump (L) and reservoir tank (G). Class A/B glass fiber filter papers (Φ1 µm) (F) were fixed inside the electrode wells to prevent soil intrusion. Molded superfine graphite rods (C, D, and E)

(0.5”OD × 12”L; Graphtek™ LLC; resistivity: 0.00050 ohm/inch) were used as electrodes because of their corrosion resistance and cost efficacy. The volume of the electrode well was 350 ml, and it was perforated to permit flow of electrolytes into the soil. Overflow tanks for the anode well (M) and cathode well (K) were connected appropriately to receive possible outflow solutions resulting from electromigration (EM) and electro-osmosis (EO) processes occurring in the system. A 3.6 kg alumina oxide ceramic surcharge plate (B) was applied on the surface of the loaded reactor to prevent possible swelling of the soil. The system was then connected to a direct current power supply (H) using electric cables (I).

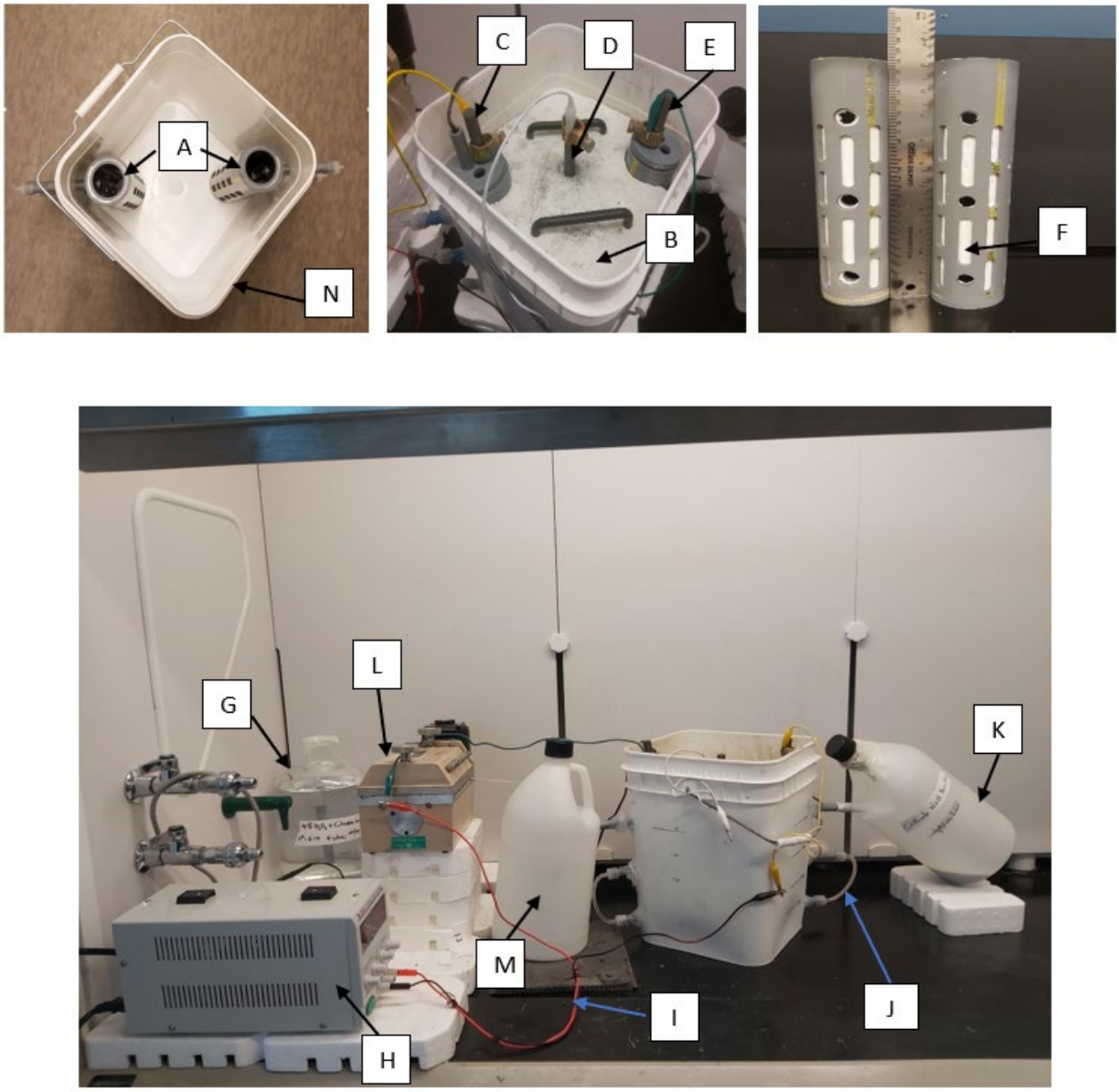

Figure 2. Photo. Bench-scale electrochemical reactor: (A) HDPE soil reactor, (B) surcharge plate, (C) anode electrode, (D) auxiliary electrode, (E) cathode electrode, (F) glass fiber filter paper, (G) reservoir, (H) direct current power supply, (I) electric cables, (J) tygon tube, (K) cathode-well overflow tank, (L) peristaltic pump, and (M) anode-well overflow tank.

Working Principle

The working principle of the reactor relies on migration of metals through EO and EM induced by an applied current. An electric gradient between the connected electrodes (i.e., the anode being positively charged and the cathode negatively charged) initiates an electrolysis reaction at both electrodes. The electrolysis reaction creates a pH gradient within the reactor, where the anode region becomes acidic with increased hydrogen ion concentration (H^+) resulting from the oxidation reaction and a release of oxygen gas. At the cathode region, an alkaline condition is created resulting from a reduction reaction producing hydroxyl ion (OH^-) and a release of hydrogen gas. As EO, electrophoresis (EP) (motion of dispersed particles) and EM processes occur within the soil, the desorbed and/or solubulized ions (or particles) migrate toward the oppositely charged electrode and create a plug flow of the soil water through the soil matrix into the overflow tanks. Electro-osmosis and EM, which are the two main processes associated with fine-grained soils, are dependent on the generation of pH and buffering capacity of the soil, the change in zeta potential of the soil particle surface, sorption and desorption of ions from the soil particle surface, oxidation-reduction reaction, and the interaction of these processes (Reddy & Cameselle, 2009). The float switch is triggered whenever there is a reduction in height of the electrode-well solution, and this initiates the peristaltic pump to refill from the reservoir. These processes are repeated throughout the duration of the reactor run.

Reactor Loading

The reactor was loaded to a total volume of 7954 cm^3, and the total mass of wet soil loaded in the reactor was 14,000 g. For the first reactor run, the soil was compacted to the in situ void ratio of 0.74 (i.e., porosity of 0.43) at 15.7% water content. For the second and third reactor runs, a preliminary soil-water trial mix was carried out to ascertain feasible compaction condition of the field soil prior to loading and adequate void ratio to permit effective fluid flow throughout the soil matrix. This was done in response to the dense state of soil and corresponding low electro-osmotic flow experienced in the lower layers of the first reactor run experiment. Twenty-five percent moisture content by dry weight of soil gave a uniform and compactible mix. The soil specimen was then prepared at a void ratio of 1.05 (i.e., porosity of 0.51) at 25% water content. Using a planetary mixer operated at 135 rpm for 5 min, 12,100 g dry soil was mixed with 1899 g water for the first reactor run, while 11,200 g dry soil and 2,800 g water were mixed for the second and third reactor runs, respectively. The soil-water mixture was compacted in the reactor in four equal thickness layers using a 2 kg hammer. Twenty-five blows were applied for each layer. Each layer was comprised of 3,500 g of soil compacted to a height of 5 cm. The compacted soil in the reactor was then covered and left for 24 hours to allow moisture equilibrium.

Chemical Reagent Selection and Application

After moisture equilibrium, both electrode wells were filled with the electrolyte solution (i.e., H_2O_2 and/or citrate buffer) until the first droplet was let out. The initial pH at both wells were the same as that of the electrolyte solution and were measured before turning on the power supply.

Illinois regulates waters more broadly than is required by the Federal Clean Water Act (ELI, 2013). For this reason, Illinois underground injection restrictions were assessed to ensure regulatory acceptance as well as to ensure that the most environmentally friendly chemical reagents were selected, as

documented in the Task 2 report (Hohner et al., 2020). H_2O_2, which was used in the first two experiments, was chosen as a catalyst to react with metal oxides in the contaminated soil and promote H_2O_2 reactions yielding reactive oxygen species (ROS), as outlined in the Task 3 report (Pelletier et al., 2021). Alternatives for H_2O_2 reactions could be iron oxides such as ferrihydrite, goethite, hematite, and magnetite, which can catalyze the decomposition of H_2O_2 to yield HO•. However, this form of catalysis functions from pH 3–7, as a function of iron speciation ($Fe^{2+} > Fe^{3+}$), iron oxide surface area, concentration, and H_2O_2 concentration (Kwan & Voelker, 2003). In addition, externally supplied soluble iron yields too rapid a rate of H_2O_2 decomposition in soils, disallowing for its transport down gradient and the necessary oxidant-contaminant contact time (Watts & Teel, 2005).

Other chemical reagents were selected based on the study with kaolinite that was reported in the Task 3 report (Pelletier et al., 2021). They include citric acid monohydrate, hydrogen peroxide (70%), and potassium hydroxide purchased from VWR Chemicals BDH; ammonium molybdate and potassium iodide from Thermo Fisher Scientific; calcium hydroxide, nitric acid, sodium hydroxide, soluble potato starch, and sulfuric acid from J.T. Baker; sodium thiosulfate from Sigma Aldrich; trisodium citrate from Research Products International; and compressed argon gas (99.985%) and ultrapure helium gas (>99.999%) from Washington State University stores.

Electrochemical Treatment Sequence

In this study, a different electrochemical treatment schedule and reagents were used for each of the three reactor runs to facilitate EM and electro-osmotic flow in the reactor. Various enhancing agents were explored to homogenously initiate the reaction and regulate the pH throughout the soil. Table 2 summarizes the electrochemical regime used in each experiment.

Table 2. Summary of Electrochemical Regime by Experiment

Exp. No.	Duration (Days)	Supplied Electrolyte		Electrical Potential	Anode Well Conditioning Solution	Cathode Well Conditioning Solution
		Anode Well	Cathode Well			
1	28	10% H_2O_2 & 0.1 M Citrate Buffer	10% H_2O_2 & 0.1 M Citrate Buffer	30 V 1.5 V/cm	1 N Potassium Hydroxide & 1 N Calcium Hydroxide	1 N Citric Acid
2	17	4% H_2O_2 & 0.1 M Citrate Buffer	4% H_2O_2 & 0.1 M Citrate Buffer	30 V 1.5 V/cm	1 N Potassium Hydroxide	1 N Citric Acid
3	14	0.1 M Citrate Buffer	0.1 M Citrate Buffer	30 V 1.5 V/cm	1 N Potassium Hydroxide	1 N Citric Acid

Reactor Performance Checks: Daily Measurements

Electrical current and electrostatic potential were measured daily between the powered-to-powered and auxiliary-to-powered electrodes using a Morpilot® auto-ranging digital multimeter. Hydrogen

peroxide concentrations in the electrode wells and reactor outflow were determined daily by sodium thiosulfate iodometric titration. The pH and temperature of electrode-well solutions and reactor outflow were measured daily with a VWR® sympHony™ B10P benchtop meter with a VWR® 89231-596 pH electrode and integrated temperature sensor in accordance with EPA Method 9045D. Ten to twenty mL liquid sample aliquots removed from the electrode wells for daily analyses were automatically replaced with fresh solution at the anode well. They were manually replaced with 10 mL fresh solution or solution recovered from the reactor outflow at the cathode well, depending on residual H_2O_2 concentration in the overflow (i.e., > 8%).

Post-treatment Experiments

After the last day of the reactor runs, the system was shut down and the treated soil was sampled for post-treatment analysis. Soil samples were collected in four layers as loaded in the reactor. For each layer, 16 sample points covering the nominal and orthogonal distance between the electrodes were used for moisture content, soil pH, and inorganic compound concentration measurements. Each layer was then mixed homogenously for geotechnical analysis (i.e., UCS, soil plasticity, etc.). Post-treatment results were compared with pretreatment measurements to evaluate the effectiveness of each reactor run.

CHAPTER 4: RESULTS AND DISCUSSION

FIRST REACTOR RUN

Pretreatment

The average pH of the sample used for the first reactor run prior to loading was in the alkaline range, with a value of 8.3. In situ moisture content was approximately 15.7%. Unconfined compressive strength (UCS) at in situ moisture content was 91.3 kPa. The liquid limit was 23, and the plasticity index was 10. This soil is classified as CL "Inorganic clays of low to medium plasticity" according to USCS (ASTM D2487). The particle size distribution curve in Figure 1 indicates the soil consists of 3% gravel, 40% sand, 44% silt, and 13% clay. Inorganic compounds of concern indicated the average contamination was 726 mg/kg for manganese and 7.9 mg/kg for arsenic. Benzo(a)pyere was initially detected in preliminary data, but upon further analysis was below the detection limit and was not included in subsequent analyses. The concentration of Mn is of concern because the maximum allowable concentrations (MACs) for Mn in the state of Illinois are specified as 636 mg/kg and 630 mg/kg within a metropolitan statistical area (MSA) and non-MSA county, respectively. For As, MACs are specified as 13 mg/kg for a MSA and 11.3 mg/kg for a non-MSA, respectively (35 IAC, part 1100 subpart F, 2012).

Post-treatment

General Observations

Outflow into the electrode well was observed on day 2. This observation may be associated with the dense state (low porosity of 0.43) at which the soil was loaded, in addition to the low permeability associated with fine-grained soils. Extreme pH at both electrode wells led to disintegration of the glass fiber filter paper placed between the fabricated HDPE electrode wells, and the pH control mechanism proved inefficient. This situation caused many complications in the overall electrochemical (EC) system, where soils migrated into the reactor well and often clogged the float switch. These complications led to non-replenishment of the solutions in the electrode wells and consequent disruption of the intended electrochemical treatment process.

pH of Electrode Wells

A spike in pH at the cathode well from 4.3 to 13.1 and a reduction in anode well pH from 4.3 to 1.2 was observed after 24 hours (Figure 3). When the pH dropped too low in the anode well, the acidic electrolyte dissolved part of the glass fiber filter and the impurities in the graphite rod, causing issues.

The following describes likely roles of the high-concentration H_2O_2 in the extremely low pH values seen in the anode well and extremely high pH values seen in the cathode well. At the anode, when acidic, $H_2O_2 \rightarrow O_2 + 2H^+ + 2e^-$ is the reduction half reaction of H_2O_2, which makes the anodic electrolyte even more acidic. The possible solutions are to reduce the concentration of H_2O_2 since there are minimal organic contaminants in the field soil to react with H_2O_2 and to increase the initial pH of the anodic electrolyte to closer to 7.0. It is cautioned that if the anodic electrolyte is alkaline (in rare cases), then the following reduction half reaction will occur: $H_2O_2 + 2OH^- \rightarrow 2H_2O + O_2 + 2e^-$.

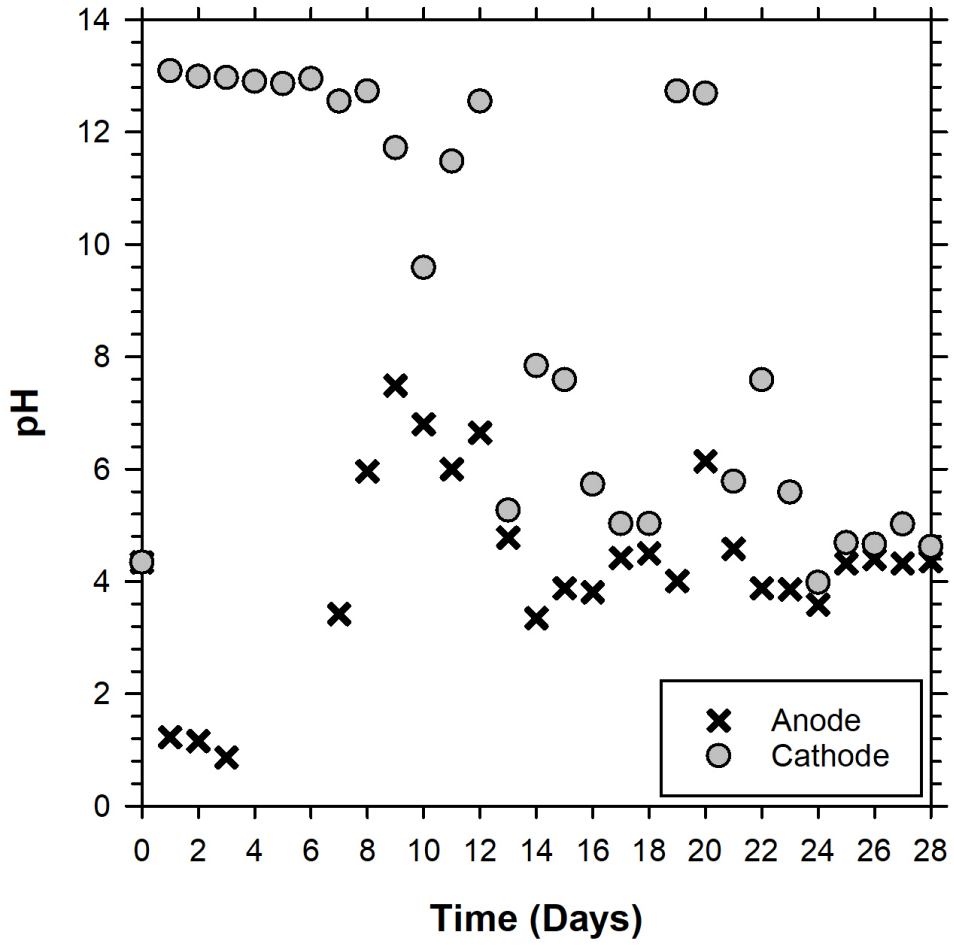

Figure 3. Graph. pH measurement at electrode wells (R1).

The changes in pH can also be attributed to the electrolysis of water producing H^+ at the anode and OH^- at the cathode, thus creating highly acidic and basic fronts, as expressed in Figure 4.

$2H_2O \rightarrow O_{2(g)} + 4H^+ + 4e^-$	Anode	$E^0 = -1.229$ V
$4H_2O + 4e^- \rightarrow 2H_{2(g)} + 4OH^-$	Cathode	$E^0 = -0.828$ V

Figure 4. Equation. Electrolysis of water at anode and cathode wells.

Reddy & Cameselle (2009)

The pH adjustment twice a day did not affect the pH in either well for the first 5 to 6 days (Figure 3). This observation may explain the disintegration of the glass fiber filter papers that permitted migration of soil grains into the electrode wells, as observed on day 5. On days 4, 5, and 6, the anode electrode well dried up from migrated soils clogging the float switch, halting the electrolyte solution replenishing the anode well while EM was still taking place.

pH of Soil Matrix

The pH distribution in the soil post-treatment shows extreme values at regions near the anode and cathode wells (Figure 5). At the region close to the anode well, the soil was observed to be acidic, while samples close to the cathode well were alkaline. Neutral pH values were observed near regions of equal distance between the anode and cathode wells across all layers. The uneven distribution in soil pH suggests that the control mechanism adopted for this reactor was inefficient to bring post-treated soil to an acceptable pH range (pH 6.25–9.0) specified by the EPA for a material to be used as a fill material (35 IAC, part 1100 subpart F, 2012). However, for field application, this pH range can be achieved by reversing the polarity on electrodes or running an alkaline solution (e.g., lime) through the soil at the end of the treatment process.

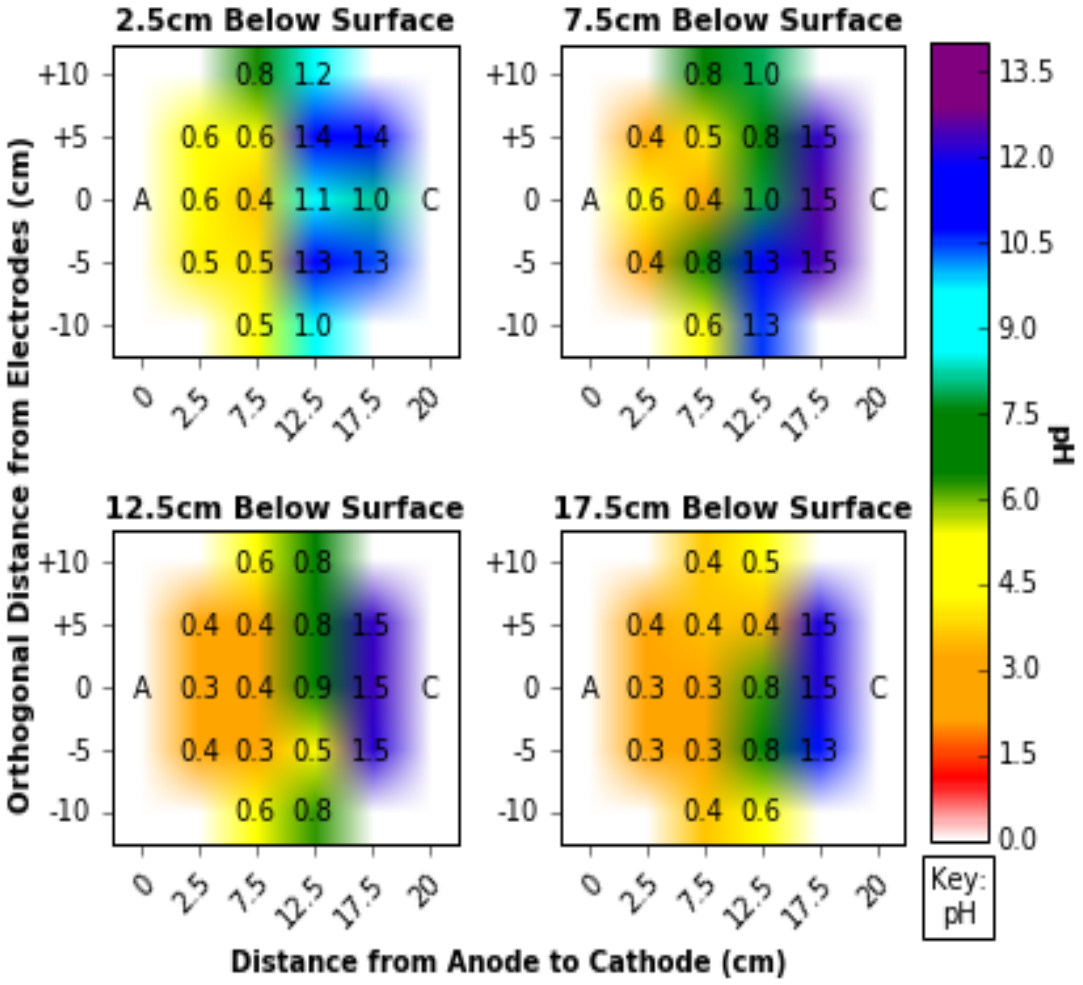

Figure 5. Graph. pH distribution of soil per layer post reactor run (R1). The numbers shown for each sample point indicate the change in pH from the initial conditions (Δ pH).

Current Density across Electrodes

Figure 6 presents the results of daily measured current flux across the reactor cell. Current density increased up to day 3 to 1.11 A followed by a subsequent decline to 0.26 A on day 11. This initial

increase was likely associated with electrolysis of water at the electrodes producing more ions in the solution and migrating through the soil pores to their respective oppositely charged electrode. The decrease after day 3 could be due to depletion in ion concentration in the reactor cell as treatment proceeded. Starting from day 12, an increase in measured current was observed with subsequent fluctuations, which is associated with dynamics in the rate of dissociation of water (electrolysis) at both electrode wells. An exception was observed on day 15, which showed an increase that may have occurred from adding fresh electrolyte solution to the system.

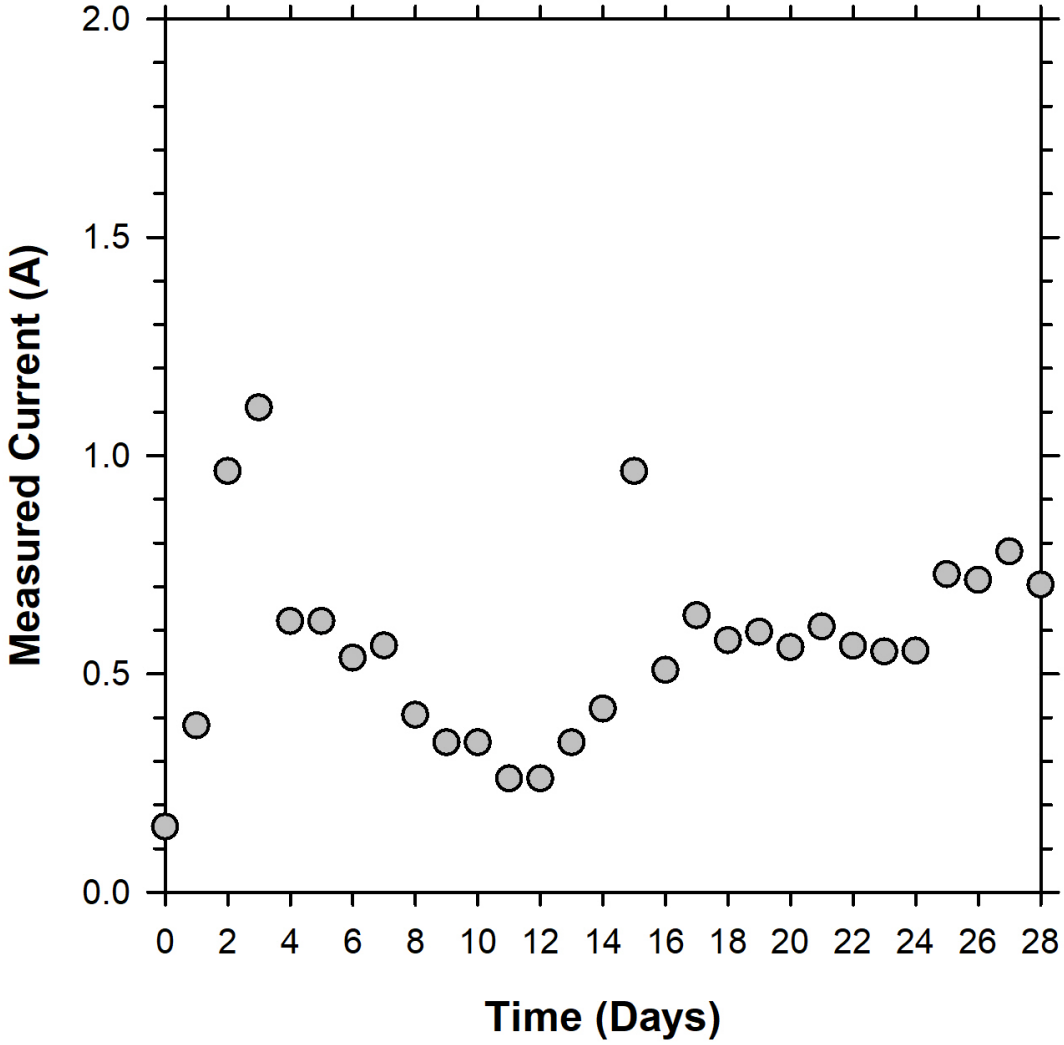

Figure 6. Graph. Daily measured current across the reactor cell (R1).

Moisture Content Distribution in the Reactor Cell

At the end of the reactor run, there was an increase in MC with depth (Figure 7). The maximum moisture content was observed near the anode well at a 12.5 cm depth below the surface (30%) and corresponds to a degree of saturation of 100%.

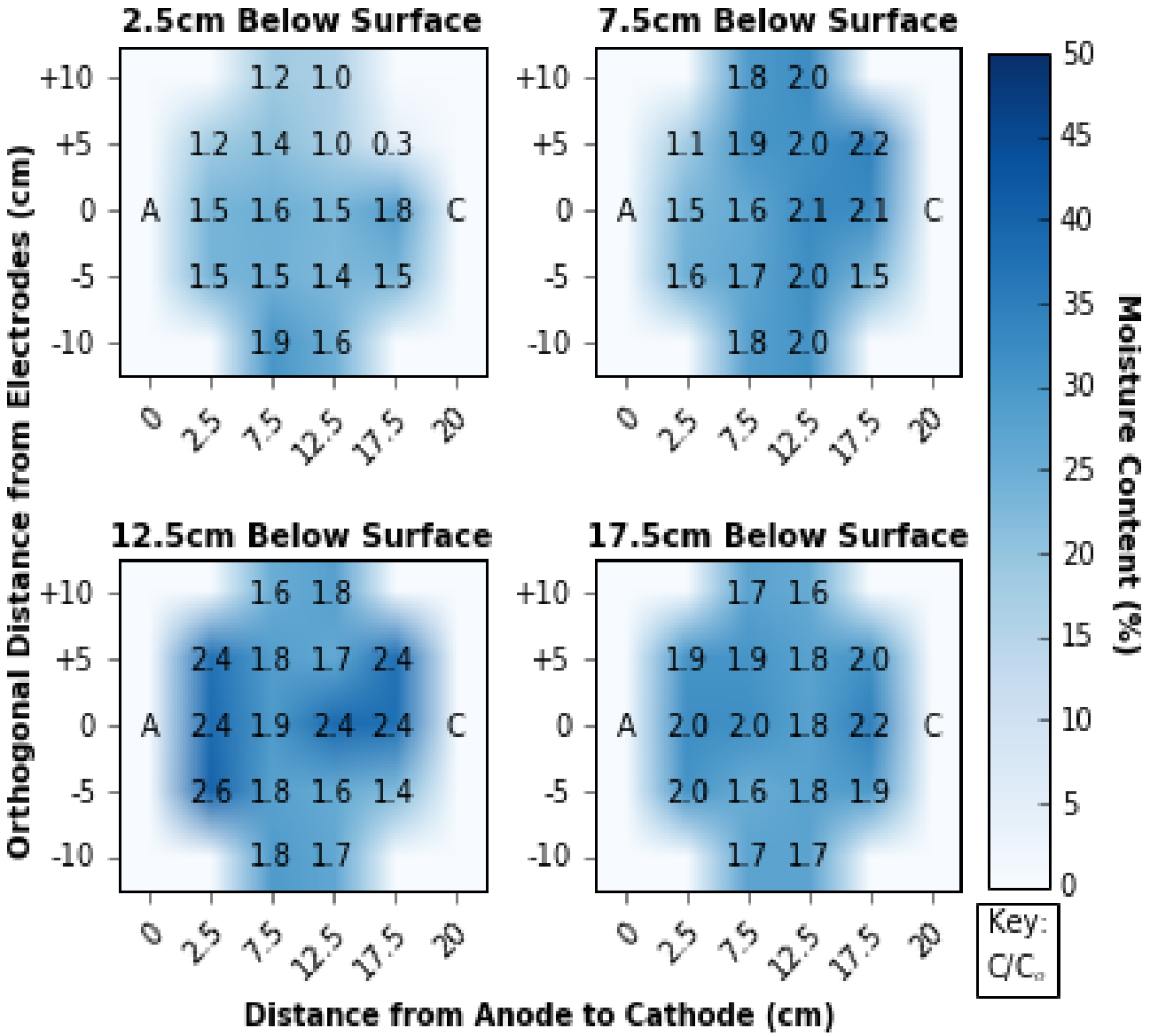

Figure 7. Graph. Moisture content distribution in soil post-treatment (R1). The numbers shown for each sample point indicate the final MC normalized by the initial MC (MC/MC_0).

Removal Efficiency of Inorganic Compounds

After a 28 day reactor run, the field soil originally containing 726 mg/kg of Mn and 7.9 mg/kg of As experienced, on average, approximately 28% and 9% extraction efficiency, respectively (Figure 8). In layers 3 and 4, the concentration of As increased in regions near the cathode well. This condition was attributed to a precipitate formation. Metals form complexes with hydroxyl ions (OH^-) in solutions with high alkalinity or high OH^- concentration (e.g., Reddy & Cameselle, 2009). As the precipitates increase in size, they become large enough to migrate downwards through the soil pores.

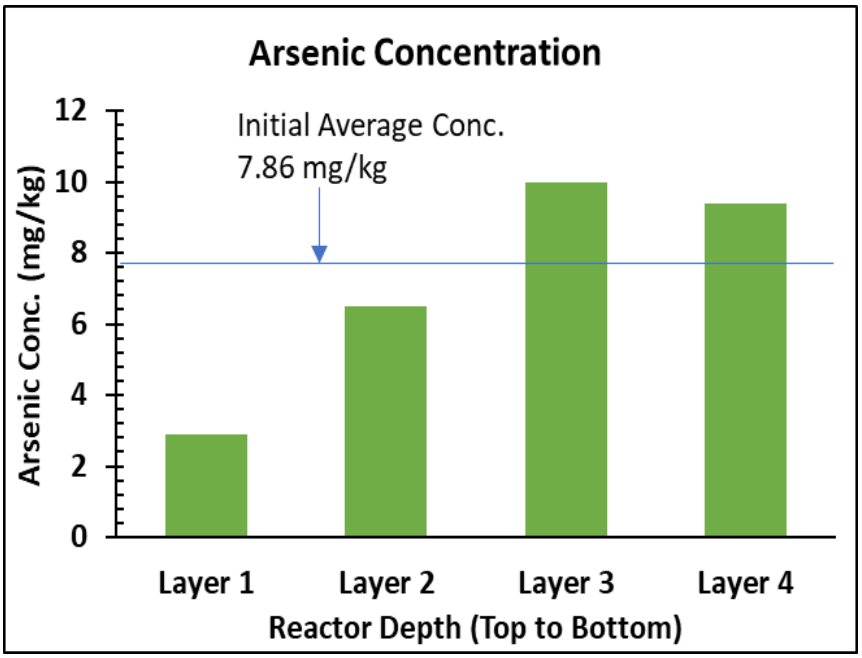

(A)

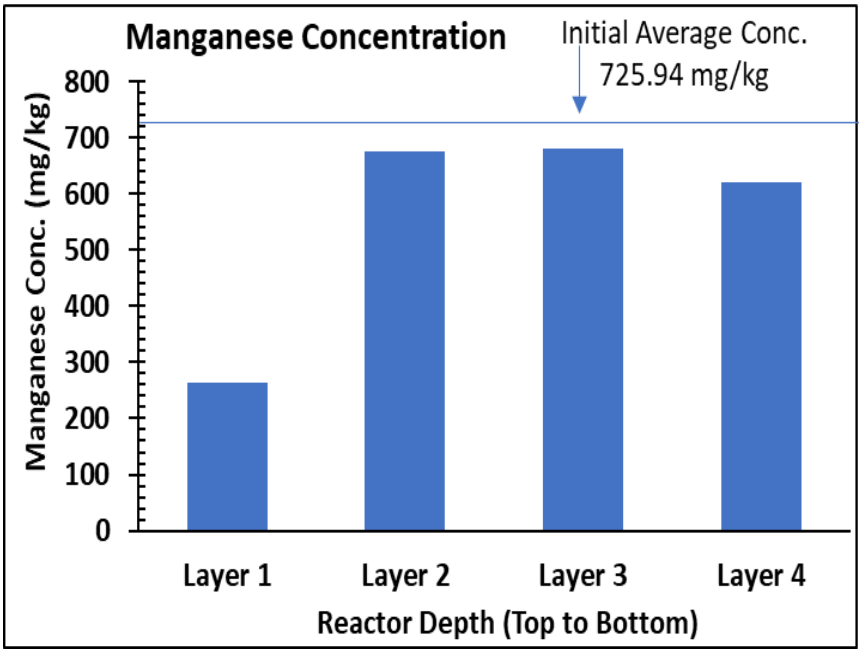

(B)

Figure 8. Graph. Inorganic compound concentration post reactor run (R1): (A) As and (B) Mn.

The change in oxidation state of As with fluctuations in pH across the reactor was interpreted to mitigate the desorption and solubilization of As, as has also been reported in past literature (e.g., Reddy & Cameselle 2009; Patrick et al., 1991). At alkaline pH conditions, As(V) is reduced to As(III), becoming more soluble and mobile for extraction. In contrast, at acidic pH range, As(III) is oxidized to As(V), becoming less soluble and mobile for efficient extraction. The pH across the reactor cell

assumed an average constant neutral value after day 5, which may contribute to the low extraction of As from the soil matrix. In contrast, Mn showed better extraction potential, suggesting a weaker bond with the soil matrix and stabilized state across a different pH range.

Soil Plasticity

Figure 9 presents soil plasticity results. Layer 1 had the lowest plasticity index of 10 post-treatment, followed by layers 2, 3, and 4 with PI of 12, 14, and 14, respectively. The plasticity of soils can be correlated with many engineering properties, including shear strength and permeability of soil (Muhunthan, 1991); hence, it is imperative to understand the influence of electrochemical treatment on the plasticity of treated soil.

Atterberg limit tests performed on the field soil pre- and post-treatment showed a direct correlation between the concentration of soil inorganic compounds and soil plasticity. Layer 1 had the lowest arsenic and manganese concentration, as evident in the inorganic compound removal results, and had the lowest PI. In contrast, layers 3 and 4 had higher concentrations of inorganic compounds arising from precipitation reactions and showed a corresponding increase in plasticity.

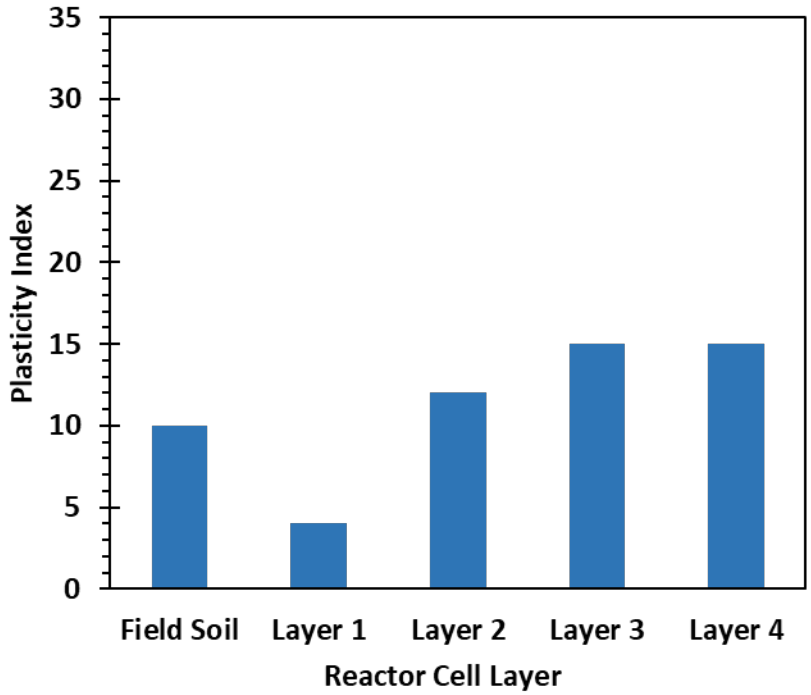

Figure 9. Graph. Soil plasticity pre- and post-treatment (R1). Pretreatment refers to the untreated field soil and post-treatment refers to layers 1–4 (treated).

Unconfined Compressive Strength

Unconfined compressive strength (UCS) of the treated soil increased in layers 2 (94 kPa), 3 (98 kPa), and 4 (101 kPa), while a decrease was observed in layer 1 (52 kPa) as compared with the untreated soil (91 kPa). The UCS results scale with soil plasticity, where layers with a higher PI exhibited a corresponding increase in UCS value (Figure 10).

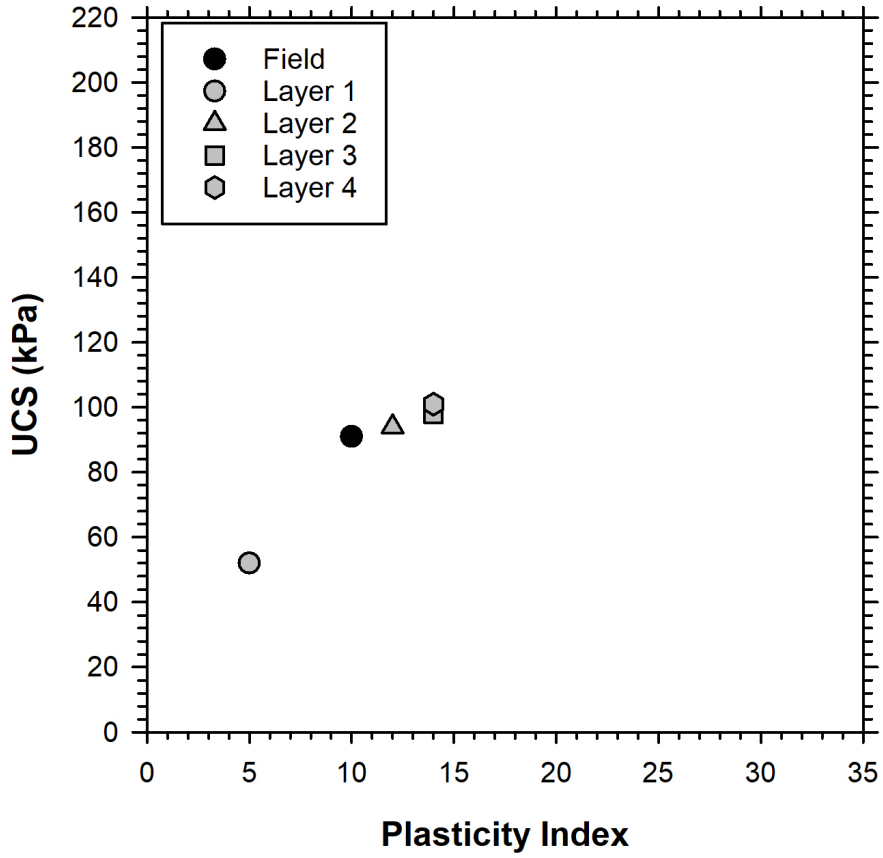

Figure 10. Graph. Soil plasticity vs unconfined compressive strength (R1).

SECOND REACTOR RUN

Pretreatment

Owing to the results obtained from the first reactor run, several changes were made for the second reactor run. These changes included reducing the concentration of hydrogen peroxide to 4% to reduce as postulated the H^+ and OH^- ion concentrations generated at the anode and cathode, respectively. In addition, the charge on the electrode was reversed for a duration of 1 hour daily after the tenth day of the reactor run to control any potential extreme pH conditions at both ends of the electrode. All pretreatment experiments performed for the first reactor run were repeated for the second reactor run. The average pH of the sample was 8.1 (n = 10). In situ moisture content was approximately 17% on average. The UCS tested at 8% moisture content was 205 kPa. The liquid limit was 44, and the plasticity index was 31. This soil was classified as CL "Inorganic clays of low to medium plasticity" according to USCS (ASTM D2487). The soil consists of 6% gravel, 30% sand, 38% silt, and 26% clay, as shown in the particle size distribution curve in Figure 1. The inorganic compounds analyzed indicated the soil contained 726 mg/kg of Mn and 7.9 mg/kg of As. Only manganese's concentration exceeds regulatory limits in the state of Illinois, as arsenic's MAC values are 13.0 mg/kg and 11.3 mg/kg by dry weight of soil within a MSA and non-MSA county, respectively.

In contrast, for Mn, the MAC values are 636 mg/kg and 630 mg/kg for MSA and non-MSA counties, respectively (35 IAC, part 1100 subpart F, 2012).

Post-treatment

General Observations

Extreme pH at both electrode wells was experienced but caused little disintegration of the glass fiber filter paper and little migration of soil into the electrode wells. The anode well dried up due to mechanical failure of the float switch but was refilled from the reservoir solution. The float switch sensor experienced a cut off resulting from contact with the wall of the electrode wells and altered continuous refilling of the anode well from the reservoir.

pH of Electrode Wells

The mechanism controlling the pH at the electrode well is the electrolysis of water. As seen in Figure 11, extreme pH conditions were recorded from day 1 with the exception of the anode well on day 2, where the electrode well dried up owing to a mechanical failure of the float switch but remained almost constant throughout the daily measurement. Reversing the charge on the electrode well for 1 hour daily helped regulate the pH at the anode well to a small degree.

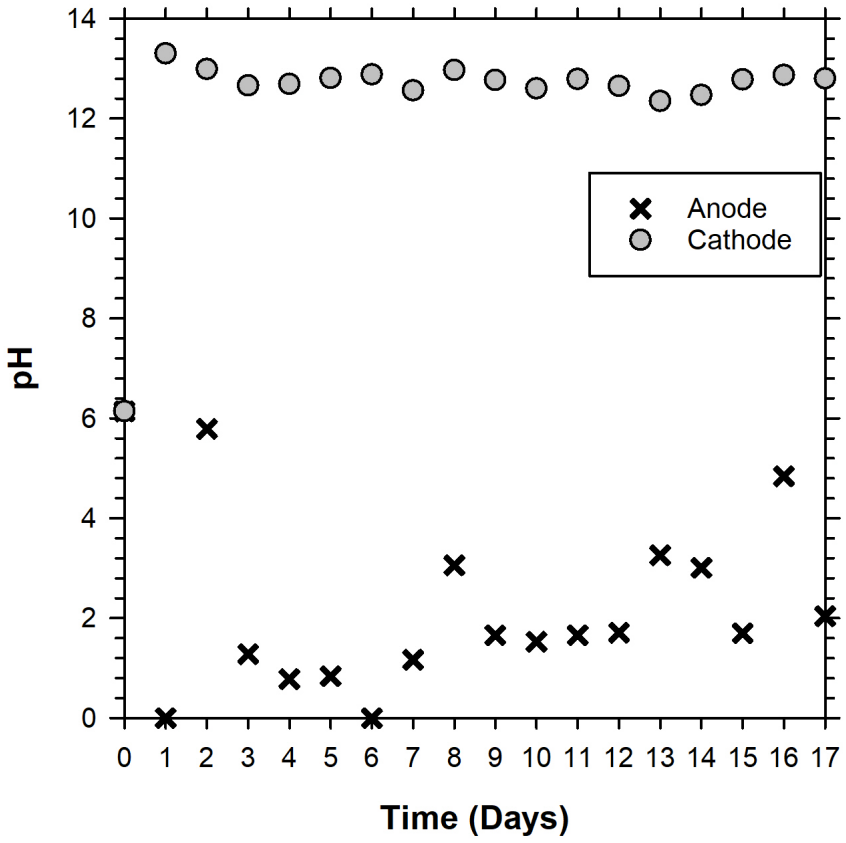

Figure 11. Graph. Daily measured pH in anode, cathode, and cathode overflow wells (R2).

pH of Soil Matrix

The post-treatment results showed that reversing the charge on electrodes for 1 hour daily effectively normalized pH in the soil matrix as compared to the conditioning solution used in the first reactor run. Figure 12 presents this improvement in pH redistribution. The pH of soils to be used as fill material in Illinois sites are required to be within 6.25–9.0 (35 IAC, part 1100 subpart F, 2012). Hence, the method of charge reversal shows positive tendencies to meet this requirement when using electrochemical techniques for soil treatment.

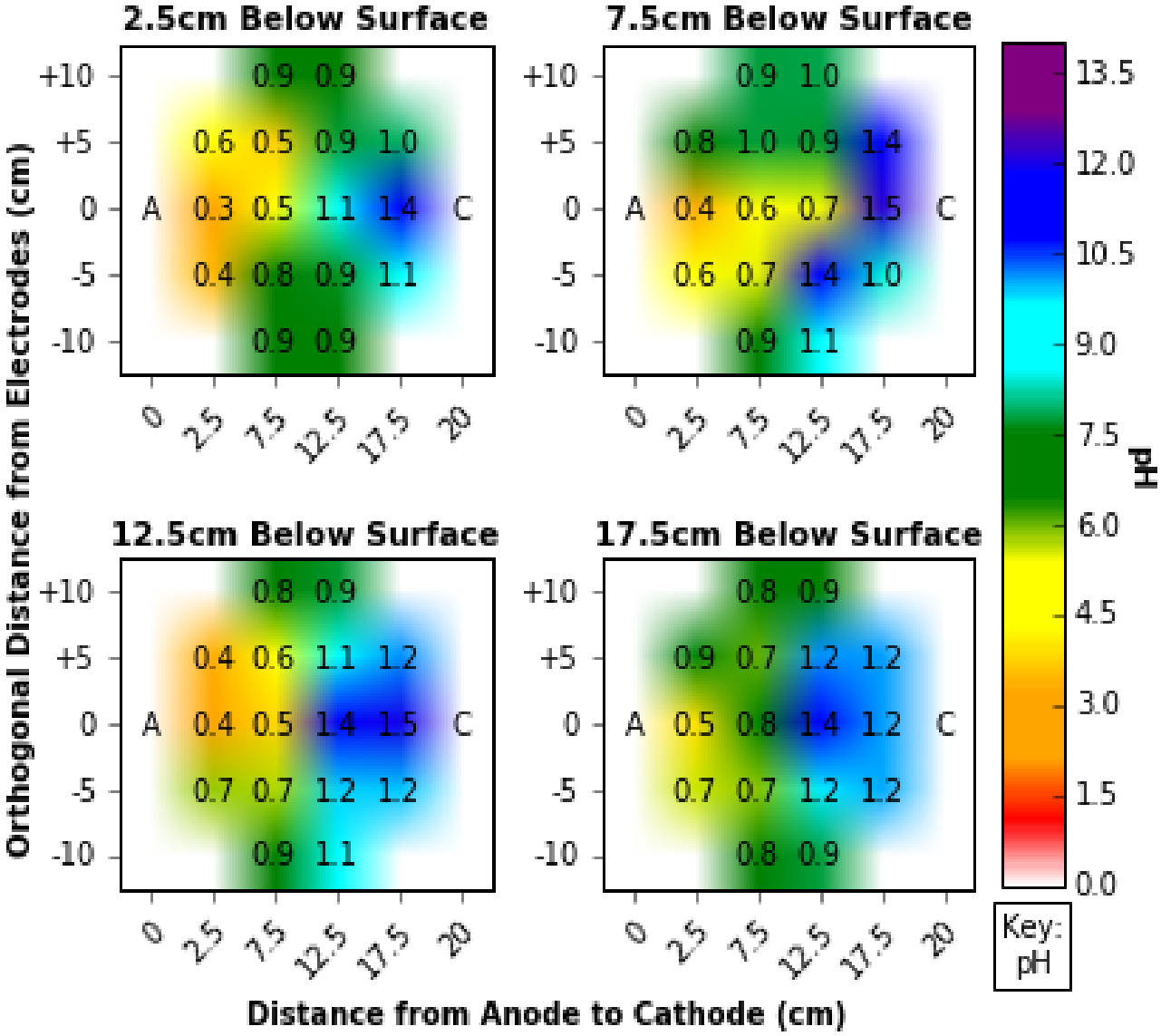

Figure 12. Graph. pH across soil matrix post-treatment (R2). The numbers shown for each sample point indicate the change in pH from the initial conditions (Δ pH).

Current Density across Electrodes

Current density measured across the electrode maintained an initial value of 0.74 A for the first two days of treatment (Figure 13). This may indicate ineffective desorption of the inorganic compounds in soil during this period. After day 2, there was a spike in the current density to 1.50 A, indicating an increase in ion concentration within the reactor cell arising from ions extracted into the pore fluids and those arising from electrolysis reactions. After day 4, the measured current decreased up to day 6 to 0.78 A and remained unchanged, on average, with little variation over time. The initial decrease was associated with effective inorganic compound extraction and migration into the cathode-well overflow tank. Afterwards, the system experienced little extraction efficiency, as reflected in subsequent current density values after day 6.

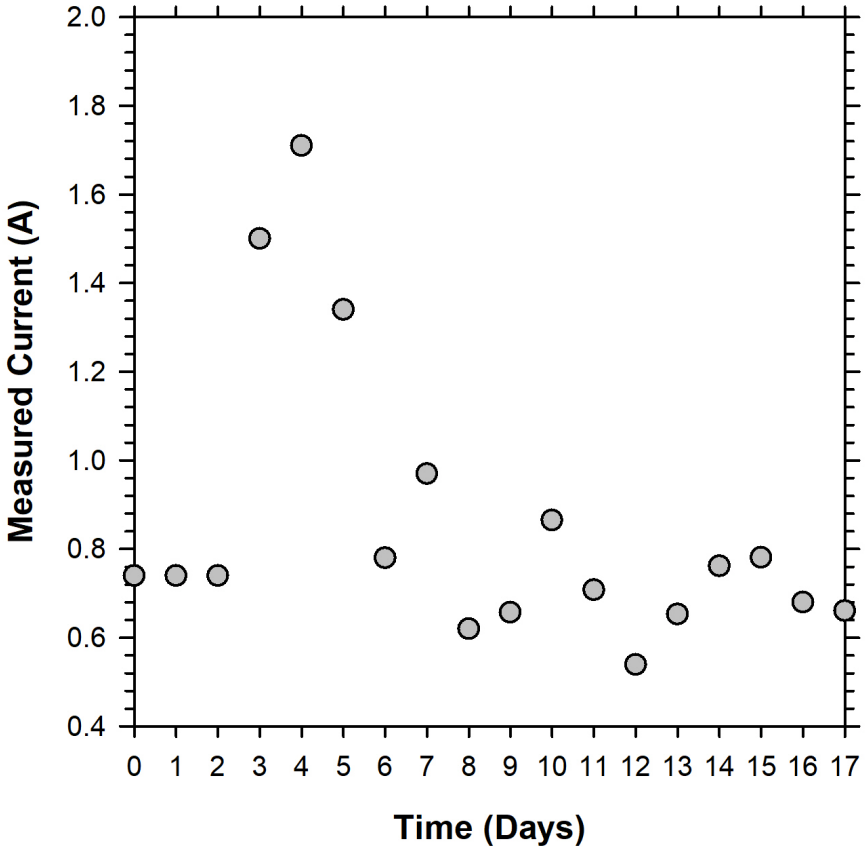

Figure 13. Graph. Daily measured current across electrodes (R2).

Moisture Content Distribution in the Reactor Cell

At the end of the reactor run, all layers showed an increase in moisture content (Figure 14). The maximum moisture content was observed at the first 2.5 cm depth below the surface (50%) and corresponds to a degree of saturation of 100%. This observation suggests more electro-osmotic flow occurred at the topmost layer. For field-scale application, the soil moisture content can be reduced by shutting down the peristaltic pump and allowing the electrolyte solution in the reactor cell to migrate toward and into the cathode outflow tank via EO.

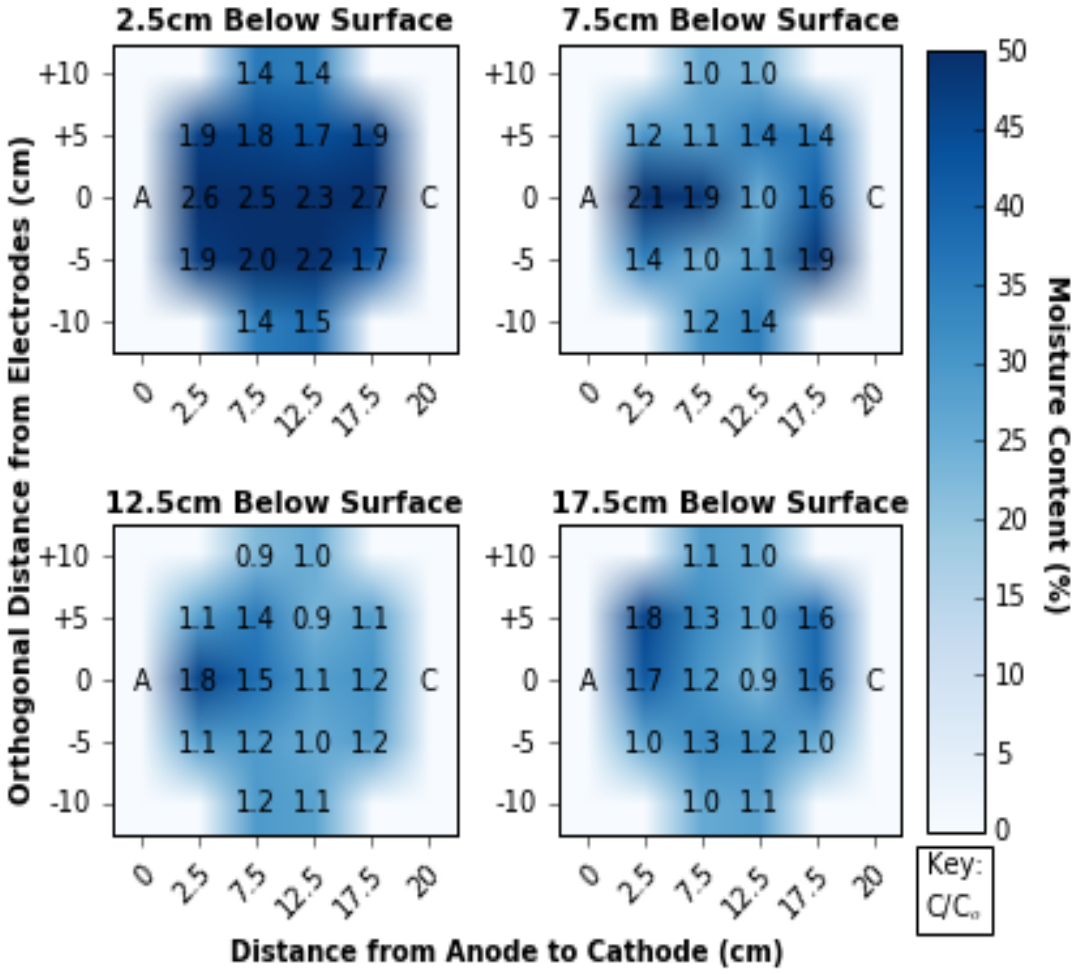

Figure 14. Graph. Moisture content distribution in soil post-treatment (R2). The numbers shown for each sample point indicate the final MC normalized by the initial MC (MC/MC_0).

Removal Efficiency of Inorganic Compounds

Prior to the second reactor run, in situ concentrations of As and Mn were measured as 7.9 and 726 mg/kg, respectively, and were used as the baseline for evaluating the extraction efficiency post-treatment. Post-treatment analysis results indicate better arsenic extraction compared to the first reactor run. The removal efficiency was 18%, 23%, 27%, and 29%, respectively, for layers 1, 2, 3, and 4 (Figure 15). Increasing the void ratio of the loaded soil increased the contact area of treatment solutions with inorganic compounds attached to the soil matrix and also facilitated increased homogenous flow in the reactor cell including the lower layers compared to that experienced in the first reactor run.

The effect of change in oxidation state of As with fluctuations in pH across the reactor also mitigated its desorption and extraction efficiency, as experienced in the first reactor run. Arsenic forms inner-sphere complexes with soil constituents (e.g., Woolson et al., 1971; Reddy & Chameselle, 2009), forming stable organic and inorganic compounds in its trivalent and pentavalent states and thus becoming difficult to desorb. In soils with oxide content, the pH regime at any time and point within

the soil matrix also affects the adsorption mechanism of the different oxidation state of As (Smith et al., 1999). The dynamics in soil pH experienced during the reactor run may have affected an effective desorption and extraction of As. Better pH control and optimization can improve this.

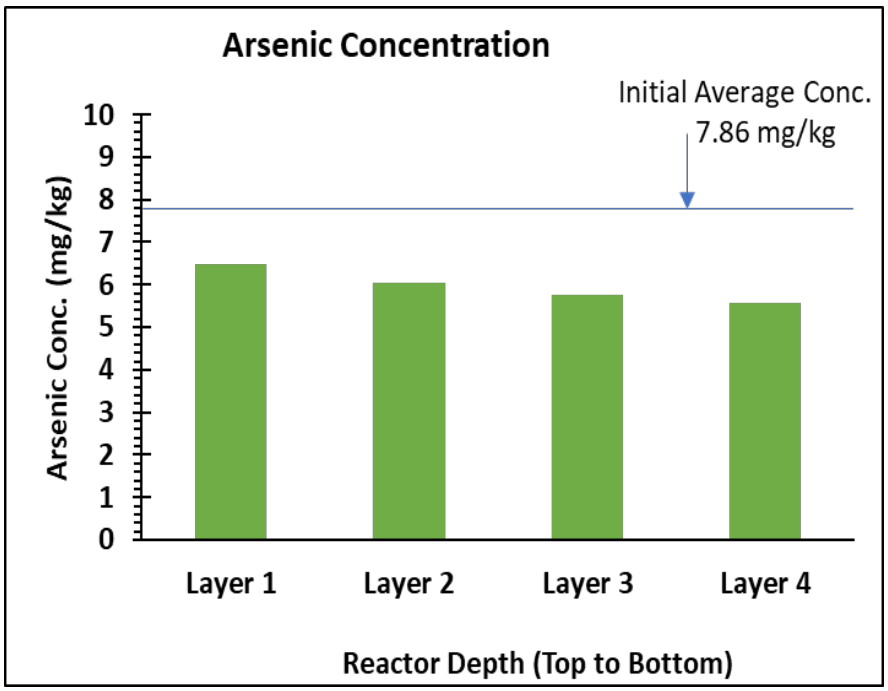

(A)

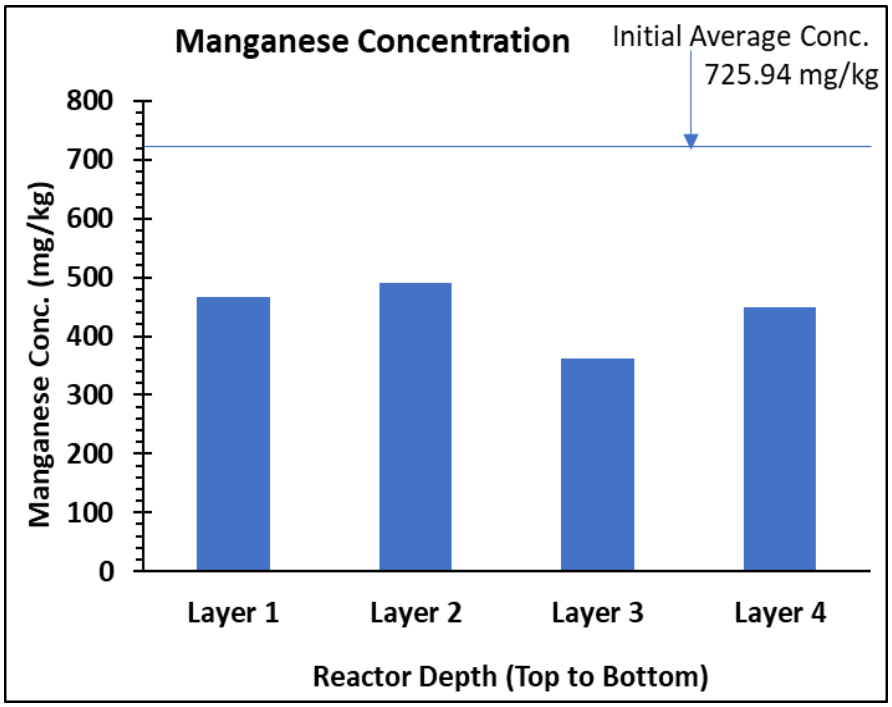

(B)

Figure 15. Graph. Contaminant concentration post reactor run (R2): (A) As and (B) Mn.

Manganese was better extracted than in the first reactor run; 36%, 34%, 52%, and 38% of Mn was effectively extracted from layers 1–4, respectively, from the field soil. The increase in soil void ratio compared to the first reactor run provided an increased contact of the adsorbed Mn with the treatment solution. This helped in desorption of Mn and increase in the electro-osmotic flow during the treatment duration. On day 6 and afterwards, results from the measured current data suggest a minimal removal efficiency. This may have resulted from a decline in Mn concentration, as extraction efficiency of inorganic compounds from soil has been postulated to be inversely proportional to their concentration. Inorganic compounds become difficult to extract from soils at low concentrations, as there is a reduction in the amount available for ion exchange (e.g., Reddy & Cameselle, 2009).

Soil Plasticity

Figure 16 presents the plasticity results post-treatment. Layer 3 had the lowest plasticity index with 18, followed by layers 2, 1, and 4, with PI of 20, 23, and 24, respectively. The results showed no direct correlation between soil plasticity and the concentration of inorganic compound of concern. This finding may suggest that the concentration of As and Mn may not be the sole mechanism controlling the soil plasticity. Other inorganic compounds present in the soil may be of interest to soil plasticity in addition to the effect of the change in treatment solution formulation (i.e., decrease in concentration of H_2O_2 from 10% to 4%).

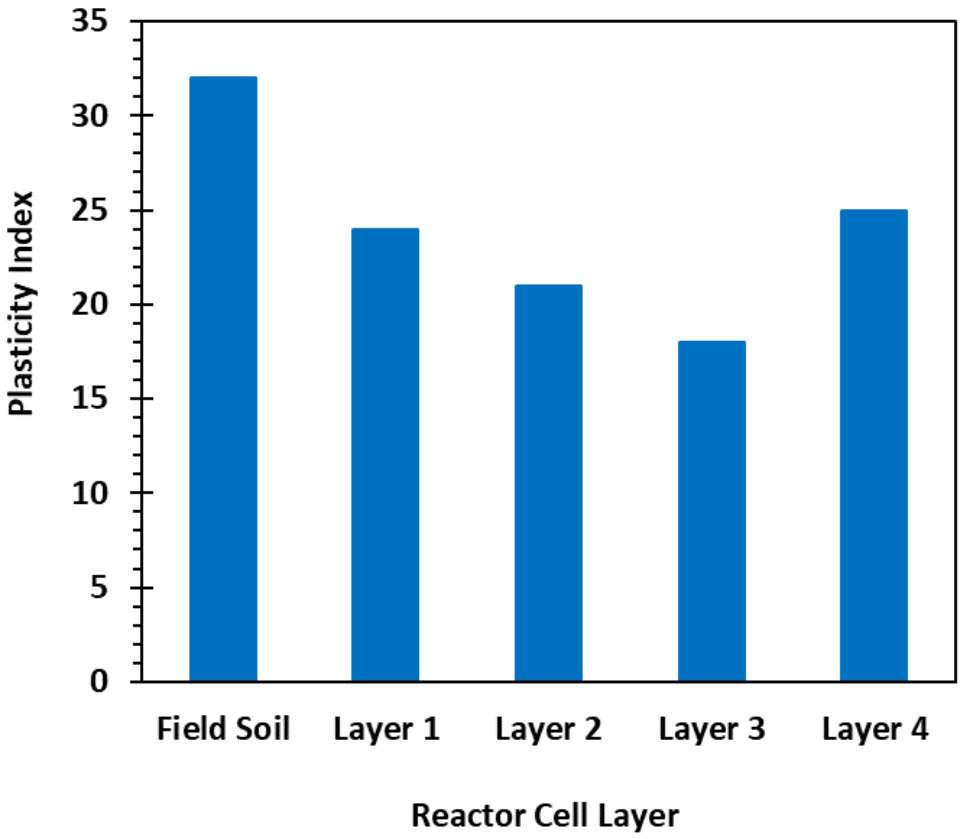

Figure 16. Graph. Soil plasticity pre- and post-treatment (R2). Pretreatment refers to the untreated field soil and post-treatment is layers 1–4 (treated).

Unconfined Compressive Strength

The UCS of the treated soil is presented in Figure 17, with values of 93, 124, 188, and 201 kPa for layers 3, 2, 1, and 4, respectively. As observed in the first reactor run, layers with a higher plasticity index exhibited a corresponding increase in the UCS value, with the exception of layer 1 (PI = 24) having a slightly lower strength than layer 4 (PI = 23).

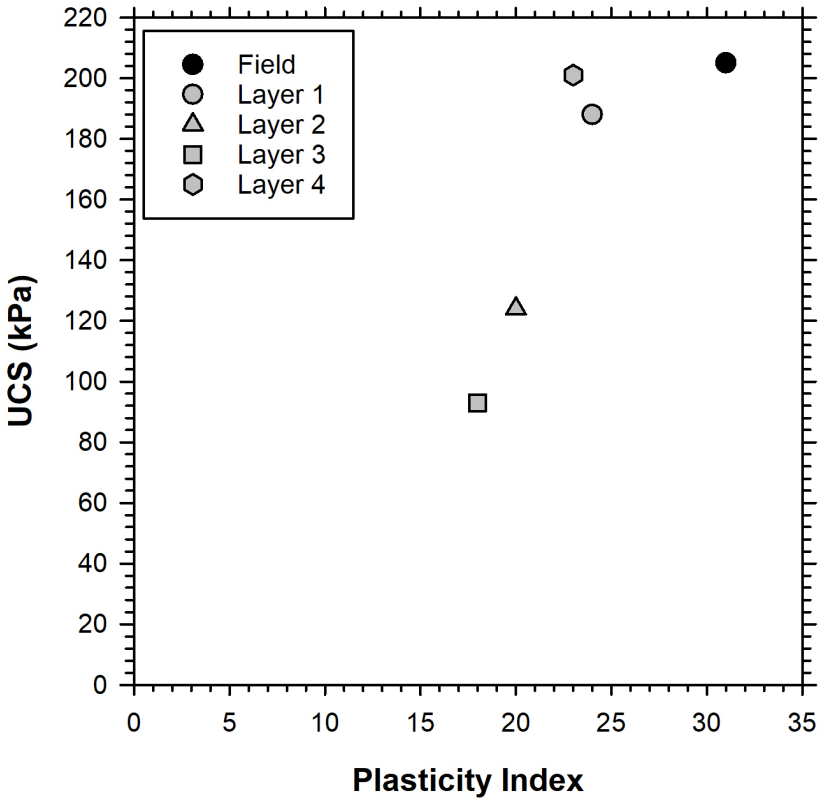

Figure 17. Graph. Soil plasticity vs unconfined compressive strength (R2).

THIRD REACTOR RUN

Pretreatment

The duration for the third reactor run was 14 days, and a 0.1 M citrate buffer solution (pH 4.5) was used as the only electrolyte solution. In addition, the charge on the electrode was reversed daily for 3 hours to control, to a larger extent, the extreme pH conditions experienced at both ends of the electrode. The average pH of the sample was 8 (n = 5), and in situ moisture content was 17%. The reactor was loaded at a moisture content of 25% with a porosity of 0.51 (void ratio 1.05). The UCS was measured at 8% moisture content as 60 kPa. Soil plasticity data showed a liquid limit value of 25, a plastic limit of 13, and a plasticity index of 12. This soil is classified as CL “Inorganic clays of low to medium plasticity” according to USCS (ASTM D2487). The particle size distribution curve in Figure 1 shows that the soil consists of 2% gravel, 35% sand, 41% silt, and 23% clay. Inorganic compounds of concern indicated the soil contained 647.8 mg/kg of Mn and 6.5 mg/kg of As. Only Mn exceeds the

regulatory limits in the state of Illinois. MAC values are 13.0 mg/kg and 11.3 mg/kg by dry weight of soil within a MSA and non-MSA county for As, respectively, while MAC values for Mn are defined as 636 mg/kg and 630 mg/kg for MSA and non-MSA counties, respectively (35 IAC, part 1100 subpart F, 2012).

Post-treatment

General Observations

There was no soil migration into the electrode wells throughout the reactor run duration. Although extreme pH conditions were also experienced at both wells, disintegration of the glass fiber filter papers were minimal compared to those experienced in the first and second reactor runs. The anode well dried up on one occasion owing to a mechanical failure of the float switch and not as a result of soil clogging. No uplift of the surcharge plate was observed, indicating the surcharge load was sufficient to curtail uplift force from possible soil swelling.

pH of Electrode Wells

Extreme spikes in pH values at the cathode and anode wells were observed after running for 24 hours (day 1), as shown in Figure 18, and similar pH values were maintained throughout the time of measurement. This observation suggests that at the electrode wells, the electrolysis of water is the dominant mechanism controlling the pH and minimal control was achieved within the electrode wells.

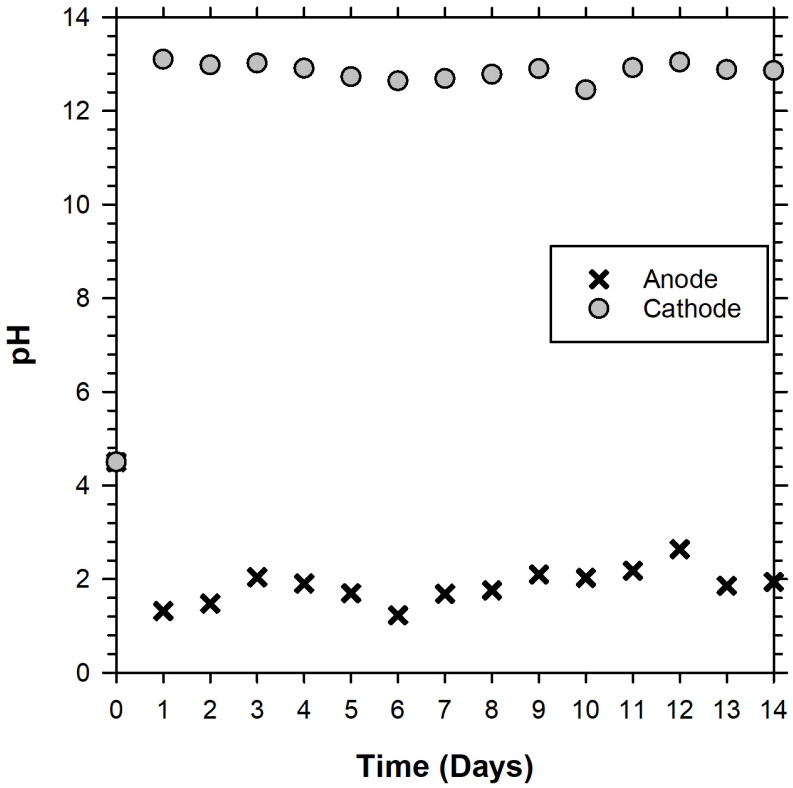

Figure 18. Graph. Daily measured pH in anode, cathode, and cathode overflow wells (R3).

pH of Soil Matrix

Post-treatment results showed that reversing the charge on electrodes for 3 hours daily better normalized pH in the soil matrix compared to conditions adopted for the first and second reactor runs. Figure 19 presents this improvement in pH redistribution. Also, pH control used in the third reactor run helped in reducing the disintegration of the anode electrode caused by extreme acidic pH conditions at the anode well.

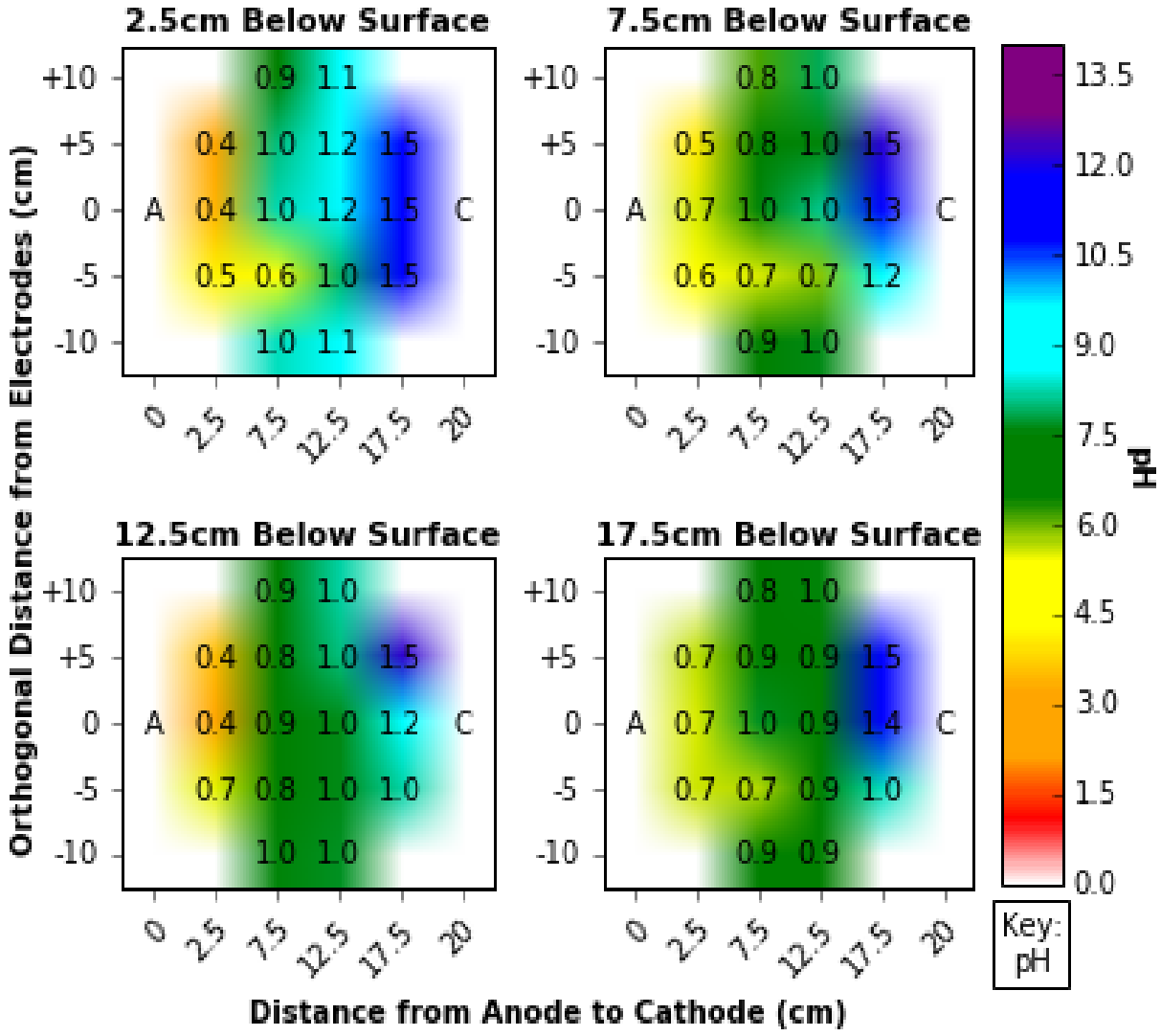

Figure 19. Graph. pH across soil matrix post-treatment (R3). The numbers shown for each sample point indicate the change in pH from the initial conditions (Δ pH).

Current Density across Electrodes

Figure 20 presents the results of daily measured current flux from anode to cathode. The current density increased when starting the reactor up to day 1 of measurement before experiencing a decline. This initial increase can be associated with ions produced from the electrolysis of water at

the electrodes and ions of inorganic compounds present in the soil matrix. The current density decreased afterward up to day 3 and attained an almost equal value for the rest of the reactor run. The decrease in current density from days 1 to 3 can likely be associated with the extraction and migration of inorganic ions from the soil into the cathode overflow tank. After day 3, the reactor experienced an almost constant current density, which may indicate little or no extraction of the inorganic compounds and might be related to the fractions that are strongly bound to the soil matrix in addition to ions produced from EO of water.

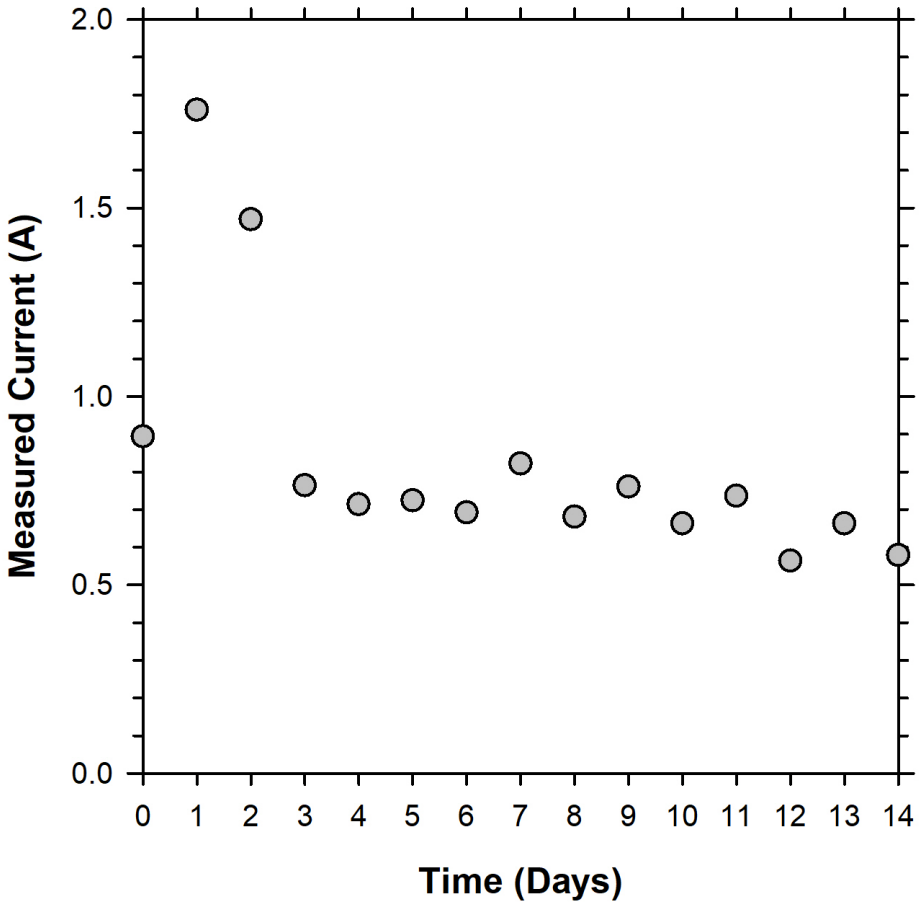

Figure 20. Graph. Daily measured current across electrodes (R3).

Moisture Content Distribution in the Reactor Cell

At the end of the reactor run, all sampled layers showed a corresponding increase in moisture content (Figure 21). The maximum MC was observed at the first 2.5 cm depth below the surface (50%) and corresponds to a degree of saturation of 100%. This finding suggests more electro-osmotic flow occurred at the topmost layer.

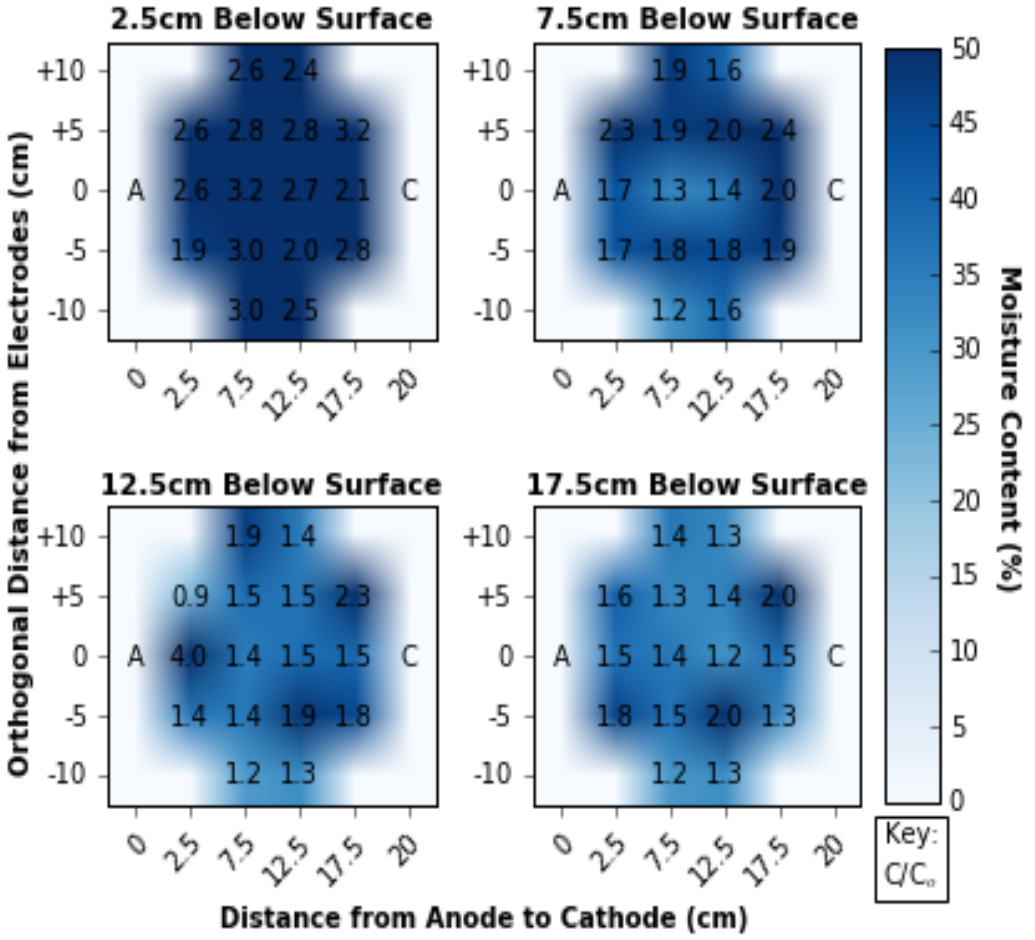

Figure 21. Graph. Moisture content distribution in soil post-treatment (R3). The numbers shown for each sample point indicate the final MC normalized by the initial MC (MC/MC_0).

Removal Efficiency of Inorganic Compounds

The soil sample used for the third reactor experiment (B-14) was analyzed using the ICPMS (KED mode) for in situ soil concentrations of As and Mn. The initial concentrations of As and Mn were 6.49 and 647.84 mg/kg, respectively. After the reactor run, the removal efficiency for As was 14%, 13%, 6%, and 5%, while Mn was 55%, 37%, 36%, 54%, respectively, for layers 1, 2, 3, and 4.

The removal efficiency of As decreased with depth from 14% to 5% (layer 1 to layer 4, Figure 22-A). Compared to the results obtained in the second reactor run, where arsenic was better removed (24% on average), superoxide radical anion ($O_2\bullet^-$) produced from the modified Fenton's reaction using 4% hydrogen peroxide and citrate buffer for the first few days might have helped to improve the desorption and solubility of arsenic. This is because $O_2\bullet^-$ acts as a surfactant, which helps to desorb and mobilize metals that are strongly bound by electrostatic forces (e.g., Watts & Teel, 2005).

On average, 49% of Mn was extracted from all layers (Figure 22-B), which is the highest removal efficiency of all reactor experiments. This finding suggests that the citric acid used in the citrate buffer solution for the third reactor run is efficient for desorbing manganese from the soil matrix. Electrical

current data obtained from the third reactor run indicates a decrease in the rate of contaminant removal after day 3.

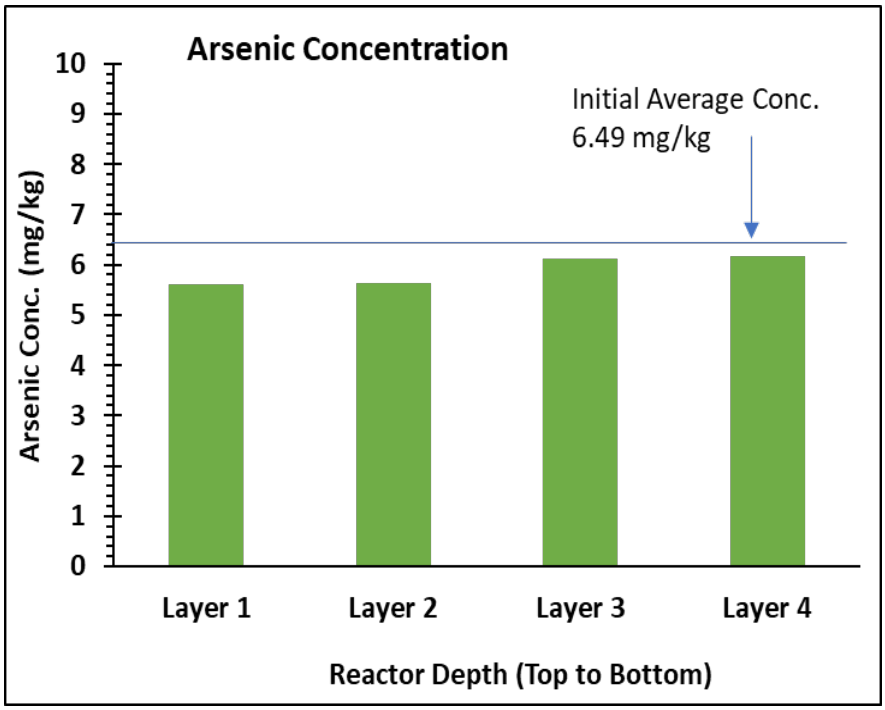

(A)

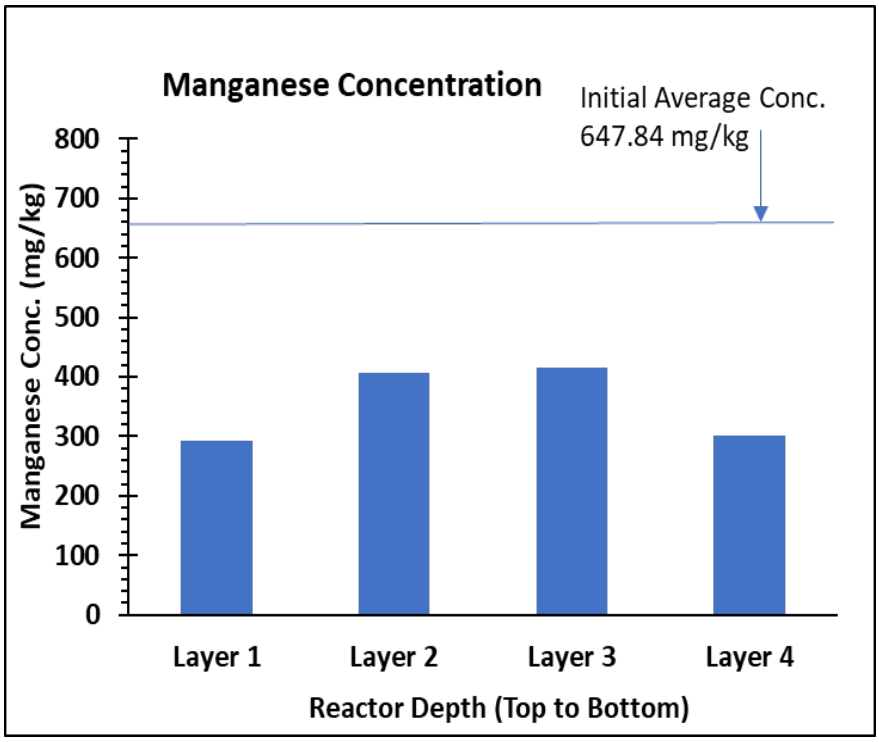

(B)

Figure 22. Graph. Contaminant concentration post reactor run (R3): (A) As and (B) Mn.

Soil Plasticity

The post-treatment analysis for the third reactor run (Figure 23) showed deviating behavior in soil plasticity correlation. Contrary to the initial postulation of increased inorganic contents with corresponding increase in plasticity, field soil with the highest concentration of inorganic compounds (6.49 mg/kg for As and 647.89 mg/kg for Mn) had the least PI (12), while layer 1 with highest removal efficiency of 14% As and 55% Mn (5.61 mg/kg As and 293 mg/kg Mn remaining in soil) had a PI of 29. This observation might indicate that As and Mn may not be the only inorganic compounds in the soil influencing soil plasticity.

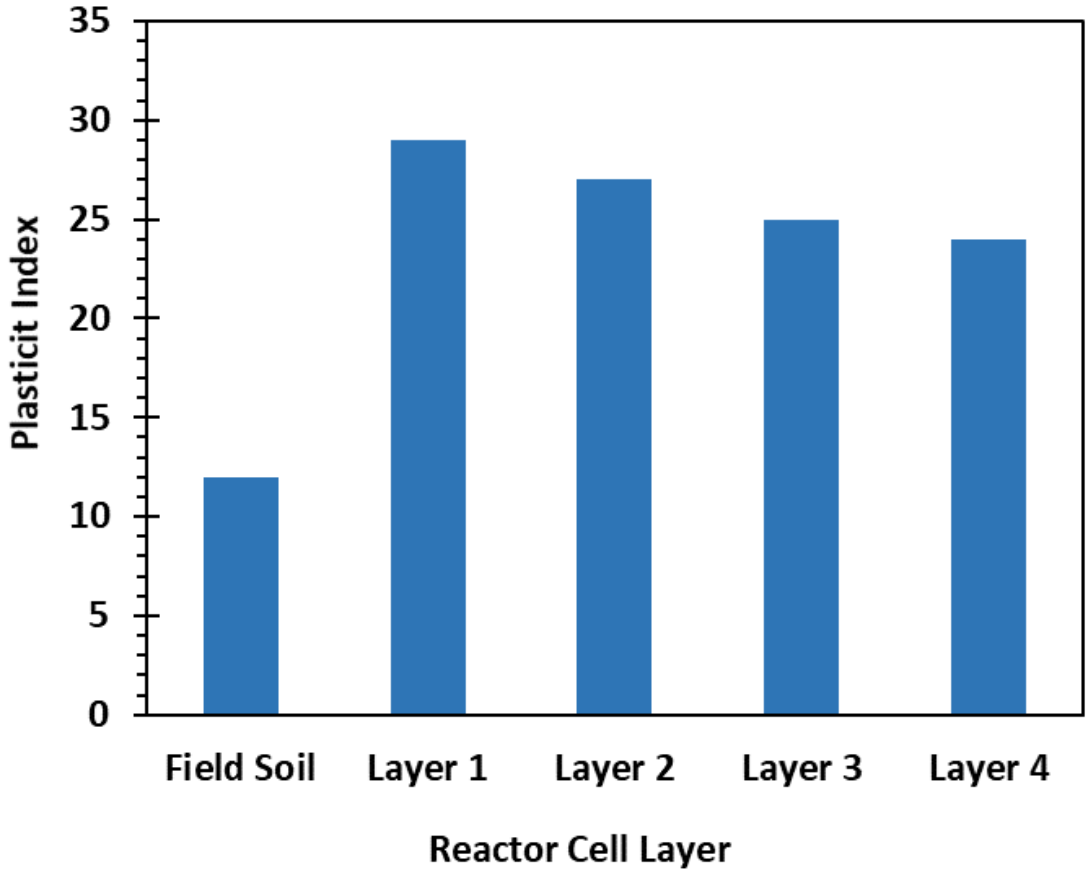

Figure 23. Graph. Soil plasticity pre- and post-treatment (R3). Pretreatment refers to the untreated field soil and post treatment is layers 1–4 (treated).

Unconfined Compressive Strength

The UCS of the treated soil was measured as 138, 105, 113, and 146 kPa for layers 1, 2, 3, and 4, respectively. The UCS value generally increased with increase in soil plasticity compared to the untreated field soil (60 kPa) but deviated for the treated soil layers (Figure 24). A general increasing trend in UCS with PI follows the trend observed in the first two reactor experiments. There was no direct correlation between the soil contaminant concentration and UCS.

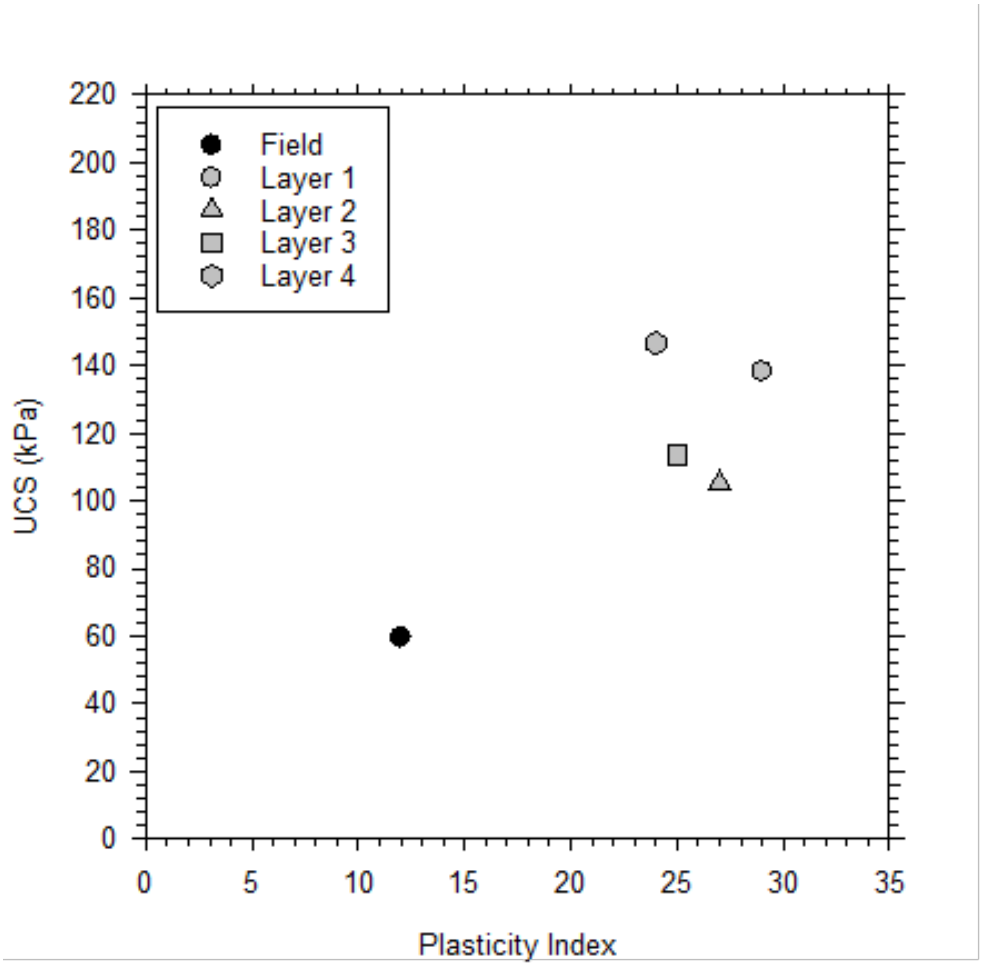

Figure 24. Graph. Soil plasticity vs unconfined compressive strength (R3).

CHAPTER 5: RESEARCH SUMMARY, CONCLUSIONS, RECOMMENDATIONS, BENEFITS, AND COSTS

RESEARCH SUMMARY

This study evaluated an accelerated in situ electrochemical treatment approach for fine-grained soils to extract inorganic compounds at a time comparable to excavation and off-site disposal. Three reactor experiments were conducted on samples collected from two borehole locations from a field site in Illinois that contained arsenic (As)(~7.4 mg/kg) and manganese (Mn)(~700 mg/kg). A combination of hydrogen peroxide (H_2O_2) and/or citrate buffer solution were used to treat the samples. A low-intensity electrical field was applied to the compacted soil samples using a bench-scale reactor resemblant of field-scale in situ EC systems. Treatment using 10% H_2O_2 and citrate buffer solution for the first reactor run resulted in an average removal of 23% and 8% for Mn and As, respectively. For the second reactor run, treatment using 4% H_2O_2 and citrate buffer achieved 39% and 24% removals for Mn and As, respectively. The third reactor run used only citrate buffer as the electrolyte, and 49% and 9% removal were achieved for Mn and As, respectively. All chemical regimes adopted in this study reduced the inorganic compound concentrations to below the maximum allowable concentration for Illinois, as specified by the Illinois administration code. The results from this work indicate that EC systems, which leverage low concentrations of hydrogen peroxide and citrate buffer, can be effective for remediating soils containing Mn and As.

CONCLUSIONS

The results from the three electrochemical soil treatment experiments demonstrated several phenomena important for the optimization of a field-scale electrochemical treatment implementation. The following conclusions were obtained:

- Arsenic showed minimal removal by the treatment process adopted. This might be a result of the dynamics in oxidation state and corresponding solubility of the various existing state of arsenic with fluctuation in soil pH. Furthermore, arsenic forms inner-sphere stable complexes with soil minerals and other organic and inorganic constituents in soils, making their desorption difficult, especially when they exist in low concentrations, as observed in this study.

- $O_2\bullet^-$ produced from H_2O_2 reactions (modified Fenton's) is hypothesized to improve desorption and solubilization of arsenic as compared to using citrate buffer alone. This is because $O_2\bullet^-$ acts as a surfactant, which may help to desorb and mobilize metals that are strongly bound by electrostatic forces (Watt & Teel, 2005).

- Citrate buffer was effective for manganese removal, with an average of 45% removal for all experiment runs. Successes in manganese extraction in fine-grained soils using citric acid have previously been reported (e.g., Genc et al., 2009; Ricart et al., 1999; Shu et al., 2015).

- The measured current data from the three reactor runs suggest that extraction efficiency was maximum for the first 3 to 5 days, after which the system experienced a decline in daily inorganic compound removal. This suggests that if treatment solution and pH is rightly optimized, then electrochemical treatment can be an effective accelerated extraction solution for inorganic compounds in fine-grained soils in less than one week of treatment.

- Alternating the charge on electrodes helped to stabilize, to a large extent, the pH through the soil profile; however, this method might reduce the electro-osmotic flow volume of the treatment solution. This reduction in electro-osmotic flow through the soil was also observed in a study by Zhang et al. (2017a).

- Soil plasticity did not show a consistent trend among the three reactor runs. Average PI stayed relatively constant after treatment for the first reactor run. Treatment resulted in a decrease in average PI after the second reactor run, whereas average PI increased after the third reactor run. Future work with controlled experiments is required to determine what caused the inconsistencies.

- Unconfined compressive strength (UCS) exhibited a consistent behavior among the three reactor runs, where a decrease in PI resulted in a general decrease in UCS.

TREATMENT RECOMMENDATIONS

The following recommendations are suggested based on results from this study:

- For better extraction of As and Mn from Illinois soils, sequential treatment may produce better results. For example, first, extract Mn using citric acid/buffer and then apply a low concentration (~4%) of H_2O_2 + citric buffer for As extraction.

- Extraction efficiency and uniformity can be achieved by optimizing cathode electrode arrangement around the anode.

- The extracted solution containing inorganics can easily be treated off site, using a precipitation method.

- Where possible, pulverizing the soil will improve the electrochemical treatment process.

RECOMMENDATIONS FOR FIELD IMPLEMENTATION

The following recommendations are suggested for field implementation under different soil organic and/or inorganic contaminant scenarios when encountered in the field:

- For the contamination with single inorganic compounds only such as arsenic, manganese, chromium, or coexistence of multiple inorganic compounds, the sequential extraction

method previously suggested is recommended if one or more compounds forms strong/inner sphere complexes with soil.

- For contamination with organic compounds only such as polycyclic aromatic hydrocarbons (PAHs) or coexistence of different organic compounds, the use of oxidants as the treatment solution such as that adopted in this study, i.e., stabilized hydrogen peroxide, is recommended.

- For mixed contamination (inorganic and organic compounds), the method adopted in this study can concurrently destroy/extract organics and inorganics. Additional sequential extraction of inorganic as previously suggested is recommended if the soil contains one or more inner sphere complex forming metal.

BENEFITS OF ELECTROCHEMICAL TREATMENT

For in situ treatment of organic and inorganic constituents in soil, EC treatments provide the following advantages:

- Treated soil can be reused on-site as construction fill material, which provides the benefit of keeping soil out of landfills that would have been generated from excavation. As a result, transportation agencies benefit from avoiding costs associated with the transport of contaminated soil long distances to landfills, treatment at the landfill, and landfill disposal fees.

- Applicable in fine-grained soils where other treatment methods are nonapplicable.

- The cost of implementing this technique will decrease with economy of scale as the treatment technology matures.

ESTIMATE OF FIELD-SCALE ELECTROCHEMICAL TREATMENT COSTS

The cost to treat approximately 250 cubic yards (191 m^3) of contaminated soil are shown in Table 3. The costs are very approximate, and a detailed cost estimate would need to be conducted on a site-by-site basis based on the type and extent of the contamination, soil types, as well as additional site-specific factors. The costs are broken down by preparation and permitting, installation and materials, and operational costs. Cost estimates for treating inorganic and organic contaminants separately are shown in Table 4 and were taken from Reddy and Cameselle (2009). As the technology matures, costs are expected to decrease.

Table 3. Approximate Cost for Treating 250 Cubic Yards (191 m^3) of Soil Co-contaminated with Organic and Inorganic Compounds

Approximate Cost Breakdown		Components
Preparation and Permitting	$15,000–$25,000 (20%)	Site Preparation Permitting Waste Management
Installation and Materials	$30,000–$50,000 (40%)	Control Panel Power Source Electrodes Electrolyte Injection Wells Electrolyte Management Unit Remediation Equipment Labor
Operation	$30,000–$50,000 (40%)	Electricity Labor Expendables, Chemicals Monitoring
Total Approximate Cost for 250 Cubic Yards		**$75,000–$125,000**
Approximate Cost per Cubic Yard Soil		**$300–$500**
Approximate Cost per Cubic Meter Soil		**$392–$654**

Table 4. Cost Summary for Electrochemical Treatment

Contaminant Class	Range ($/$m^3$)	Average ($/$m^3$)	Range ($/cubic yard)	Average ($/cubic yard)
Inorganic	115–400	200	88–306	153
Organic	90–275	200	69–210	153

Reddy & Cameselle (2009)

REFERENCES

Acar, Y. B., Gale, R. J., Putnam, G. A., Hamed, J., & Wong, R. L. (1990). Electrochemical processing of soils: Theory of pH gradient development by diffusion, migration, and linear convection. *Journal of Environmental Science & Health Part A*, *25*(6), 687–714. https://doi.org/10.1080/10934529009375590

Adewunmi, W. (2019). Drummer Illinois State Soil. Retrieved from Soil Science Society of America website: https://www.soils4teachers.org/files/s4t/k12outreach/il-state-soil-booklet.pdf

Alcántara, M. T., Gómez, J., Pazos, M., & Sanromán, M. A. (2008). Combined treatment of PAHs contaminated soils using the sequence extraction with surfactant–electrochemical degradation. *Chemosphere*, *70*(8), 1438–1444. https://doi.org/10.1016/j.chemosphere.2007.08.070

Ammami, M. T., Portet-Koltalo, F., Benamar, A., Duclairoir-Poc, C., Wang, H., & Le Derf, F. (2015). Application of biosurfactants and periodic voltage gradient for enhanced electrokinetic treatment of metals and PAHs in dredged marine sediments. *Chemosphere*, *125*, 1–8. https://doi.org/10.1016/j.chemosphere.2014.12.087

ASTM D2487-11. (2017). *Standard practice for classification of soils for engineering purposes (Unified Soil Classification System)*. Annual Book of ASTM Standards, ASTM International.

ASTM D2216-19. (2019). *Standard test methods for laboratory determination of water (moisture) content of soil and rock by mass*. Annual Book of ASTM Standards, ASTM International.

ASTM D4318-17. (2019). *Standard test methods for liquid limit, plastic limit, and plasticity index of soils*. Annual Book of ASTM Standards, ASTM International.

ASTM D6913. (2004). *Standard test methods for particle-size distribution (gradation) of soils using sieve analysis*. Annual Book of ASTM Standards, ASTM International.

ASTM D7928. (2017). *Standard test method for particle-size distribution (gradation) of fine-grained soils using the sedimentation (hydrometer)*. Annual Book of ASTM Standards, ASTM International.

Butterfield, R., & Johnston, I. W. (1980). The influence of electroosmosis on metallic piles in clay. *Geotechnique*, *30*(1), 17–37. https://doi.org/10.1680/geot.1980.30.1.17

Chappell, B. A., & Burton, P. L. (1975). Electroosmosis applied to unstable embankment. *Journal of the Geotechnical Engineering Division*, *101*(8), 733–740.

Diamond, M. L., & Hodge, E. (2007). Urban contaminant dynamics: From source to effect. *Environmental Science and Technology*, *41*(11), 3796–3800.

Duan, L., Naidu, R., Thavamani, P., Meaklim, J., & Megharaj, M. (2015). Managing long-term polycyclic aromatic hydrocarbon contaminated soils: A risk-based approach. *Environmental Science and Pollution Research*, *22*(12), 8927–8941. https://doi.org/10.1007/s11356-013-2270-0

ELI. (2013). *ELI state constraints study (May 2013)* [ELI 50-State Study]. Environmental Law Institute.

Esrig, M. I. (1978). Increasing offshore pile drivability through electroosmosis. Paper presented at the Offshore Technology Conference, Houston, Texas, May 1978. https://doi.org/10.4043/3269-MS

Genc, A., Chase, G., & Foos, A. (2009). Electrokinetic removal of manganese from river sediment. *Water, Air, and Soil Pollution*, *197*(1–4), 131–141. https://doi.org/10.1007/s11270-008-9796-7

Hohner, A. K., Pelletier, A., Akin, I., Chowdhury, I., Watts, R., Shi, X., Dutmer, B., & Mueller, J. (2020). *Summary of Illinois regulations and review of treatment alternatives for contaminated soils in right-of-ways* (Report No. FHWA-ICT-20-010). Illinois Center for Transportation. https://doi.org/10.36501/0197-9191/20-016

ICT. (2018, February 8). *R27-183: Evaluation of On-Site and In situ Treatment Alternatives for Contaminated Soils: Kickoff Meeting Minutes*. Illinois Center for Transportation.

Illinois Administrative Code, 35 IAC Part 1100 subpart F (2012). AUTHORITY: Implementing Sections 5, 3.160, 22.51, and 22.51a and authorized by Sections 3.160, 22.51, 22.51a, and 27 of the Environmental Protection Act [415 ILCS 5/5, 22.51, 22.51a, and 27]. SOURCE: Adopted in R06-19 at 30 Ill. Reg.14534, effective August 24, 2006; amended in R12-9 at 36 Ill. Reg. 13892, effective August 27, 2012. http://www.ilga.gov/commission/jcar/admincode/035/03501100sections.html

Isosaari, P., & Sillanpää, M. (2012). Effects of oxalate and phosphate on electrokinetic removal of arsenic from mine tailings. *Separation and Purification Technology*, *86*, 26–34. https://doi.org/10.1016/j.seppur.2011.10.016

Jeyakanthan, V., Gnanendran, C. T., & Lo, S. C. (2011). Laboratory assessment of electro-osmotic stabilization of soft clay. *Canadian Geotechnical Journal*, *48*(12), 1788–1802. https://doi.org/10.1139/t11-073

Kim, S. O., & Kim, K. W. (2001). Monitoring of electrokinetic removal of inorganic compounds in tailing-soils using sequential extraction analysis. *Journal of Hazardous Materials*, *85*(3), 195–211. https://doi.org/10.1016/S0304-3894(01)00211-4

Kwan, W. P., & Voelker, B. M. (2003). Rates of hydroxyl radical generation and organic compound oxidation in mineral-catalyzed Fenton-like systems. *Environmental Science & Technology*, *37*(6), 1150–1158. https://doi.org/10.1021/es020874g

Merian, E., Anke, M., Ihnat, M., & Stoeppler, M. (2004). *Elements and their compounds in the environment: Occurrence, analysis, and biological relevance* (2nd ed). Wiley-VCH Verlag GmbH & Co. KGaA.

Mitchell, J. K., & Wan, T-Y. (1977). Electroosmotic consolidation: Its effects on soft soils. *Proceedings of the IX ICSMFE*, Tokyo, Vol. 1, pp. 219–224.

Muhunthan, B. (1991). Liquid limit and surface area of clays. *Geotechnique*, *41*(1), 135–138. https://doi.org/10.1680/geot.1991.41.1.135

Ottosen, L. M., Hansen, H. K., Ribeiro, A. B., & Villumsen, A. (2001). Removal of Cu, Pb and Zn in an applied electric field in calcareous and non-calcareous soils. *Journal of Hazardous Materials*, *85*(3), 291–299. https://doi.org/10.1016/S0304-3894(01)00231-X

Pamukcu, S., & Wittle, J. K. (1994). Electrokinetically enhanced in situ soil decontamination. *Treatment of Hazardous Waste Contaminated Soils*, 245–298.

Patnaik, P. (2007). *A comprehensive guide to the hazardous properties of chemical substances*. John Wiley & Sons.

Patrick, H. M., Ronald, D. D., & William, H. P., Jr. (1991). Effect of redox potential and pH on arsenic speciation and solubility in a contaminated soil. *Environ. Sci. Technol*., *25*, 1414–1419.

Pelletier, A., Hohner, A., Akin, I., Chowdhury, I., Watts, R., Shi, X., & Mueller, J. (2021). *Bench-scale electrochemical treatment of co-contaminated clayey soil* (Report No. FHWA-ICT-21-018). Illinois Center for Transportation.

Reddy, K. R., & Cameselle, C. (2009). *Electrochemical treatment technologies for polluted soils, sediments, and groundwater*. John Wiley & Sons, Inc.

Ricart, M. T., Cameselle, C., Lucas, T., & Lema, J. M. (1999). Manganese removal from spiked kaolinitic soil and sludge by electromigration. *Separation Science and Technology*, *3*(16), 3227–3241. https://doi.org/10.1081/SS-100100832

Shu, J., Liu, R., Liu, Z., Du, J., & Tao, C. (2015). Electrokinetic treatment of manganese and ammonia nitrogen from electrolytic manganese residue. *Environmental Science and Pollution Research*, *22*(20), 16004–16013. https://scite.ai/reports/10.1007/s11356-015-4817-8

Smith, E., Naidu, R., & Alston, A. M. (1999). Chemistry of arsenic in soils: I. Sorption of arsenate and arsenite by four Australian soils. *Journal of Environmental Quality*, *28*(6), 1719–1726. https://doi.org/10.2134/jeq1999.00472425002800060005x

United States Department of Agriculture. (2015). Drummer Series. Website for Official Soil Series Descriptions and Series Classification Retrieved December 24, 2020, from https://soilseries .sc.egov.usda.gov/OSD_Docs/D/DRUMMER.html

USEPA, Office of Solid Waste and Emergency Response. EPA/SQO/R-95/036. Updated Quarterly. Amended at 25 Ill. Reg. 10374, effective August 15, 2001.

USEPA. (2021). Method 3050B Acid Digestion of Sediments, Sludges, and Soils. United States Environmental Protection Agency. Retrieved May 19, 2021 from, https://www.epa.gov/sites /production/files/2015-06/documents/epa-3050b.pdf

Watts, R. J., & Teel, A. L. (2005). Chemistry of modified Fenton's reagent (catalyzed H_2O_2 propagations–CHP) for in situ soil and groundwater treatment. *Journal of Environmental Engineering*, *131*(4), 612–622. https://doi.org/10.1061/(ASCE)0733-9372(2005)131:4(612)

Woolson, E. A., Axley, J. H., & Kearney, P. C. (1971). The chemistry and phytotoxicity of arsenic in soils: I. Contaminated field soils. *Soil Science Society of America Journal*, *35*(6), 938–943. https://doi.org/10.2136/sssaj1971.03615995003500060027x

Yuan, C., & Chiang, T. S. (2008). Enhancement of electrokinetic treatment of arsenic spiked soil by chemical reagents. *Journal of Hazardous Materials*, *152*(1), 309–315. https://doi.org/10.1016/j.jhazmat.2007.06.099

Yukawa, H., Kobayashi, K., Tsukuf, Y., Yamano, S., & Iwata, M. (1976). Analysis of batch electrokinetic filtration. *Journal of Chemical Engineering of Japan*, *9*(5), 396–401. https://doi.org/10.1252/jcej.9.396

Zhang, H., Zhou, G., Wu, J., Zhong, J., Wu, J., & Shi, X. (2017a). Mechanism for soil reinforcement by electroosmosis in the presence of calcium chloride. *Chemical Engineering Communications*, *204*(4), 424–433. https://doi.org/10.1080/00986445.2016.1273833

Zhang, H., Zhou, G., Zhong, J., Shen, Z., & Shi, X. (2017b). Effect of nanomaterials and electrode configuration on soil consolidation by electroosmosis: Experimental and modeling studies. *Rsc Advances*, *7*(20), 12103–12112. https://doi.org/10.1039/C6RA26674F

Zhang, M., Guo, P., Wu, B., & Guo, S. (2020). Change in soil ion content and soil water-holding capacity during electro-biotreatment of petroleum contaminated saline soil. *Journal of Hazardous Materials*, *387*, 122003. https://doi.org/10.1016/j.jhazmat.2019.122003

APPENDIX A: FIELD SAMPLING

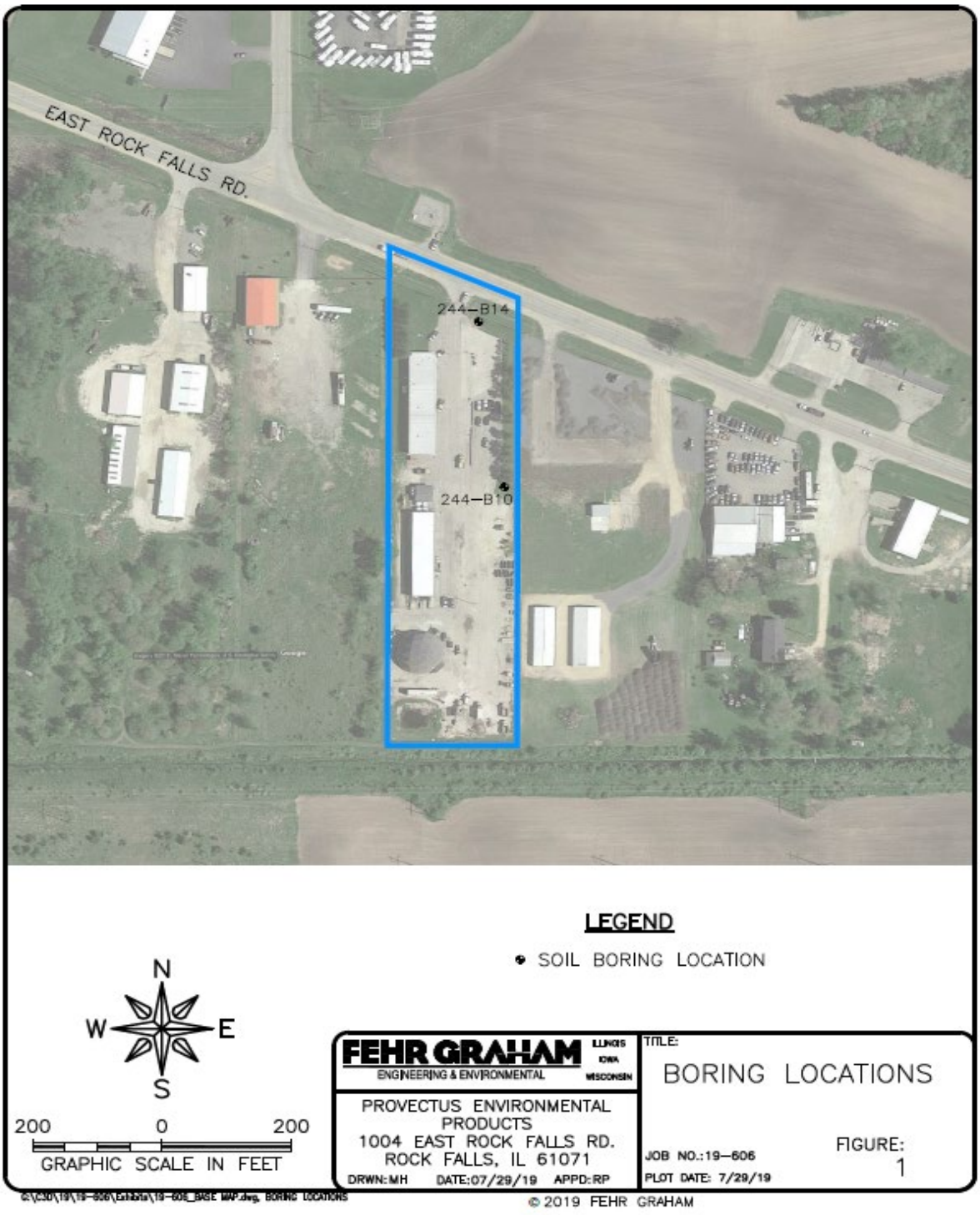

Figure 25. Photo. Field soil boring location.



(A) Boring 244-B14, facing east



(B) Boring 244-B14, facing south

Figure 26. Photos. Rock Falls sample collection borings for B14 soil (Yard 244 @ 1004 E. Rock Falls Road / Rt 30, Rock Falls, Illinois).



(A) Boring 244-B10, facing east



(B) Boring 244-B10, facing south

Figure 27. Photos. Rock Falls sample collection borings for the B10 soil (Yard 244 @ 1004 E. Rock Falls Road / Rt 30, Rock Falls, Illinois).

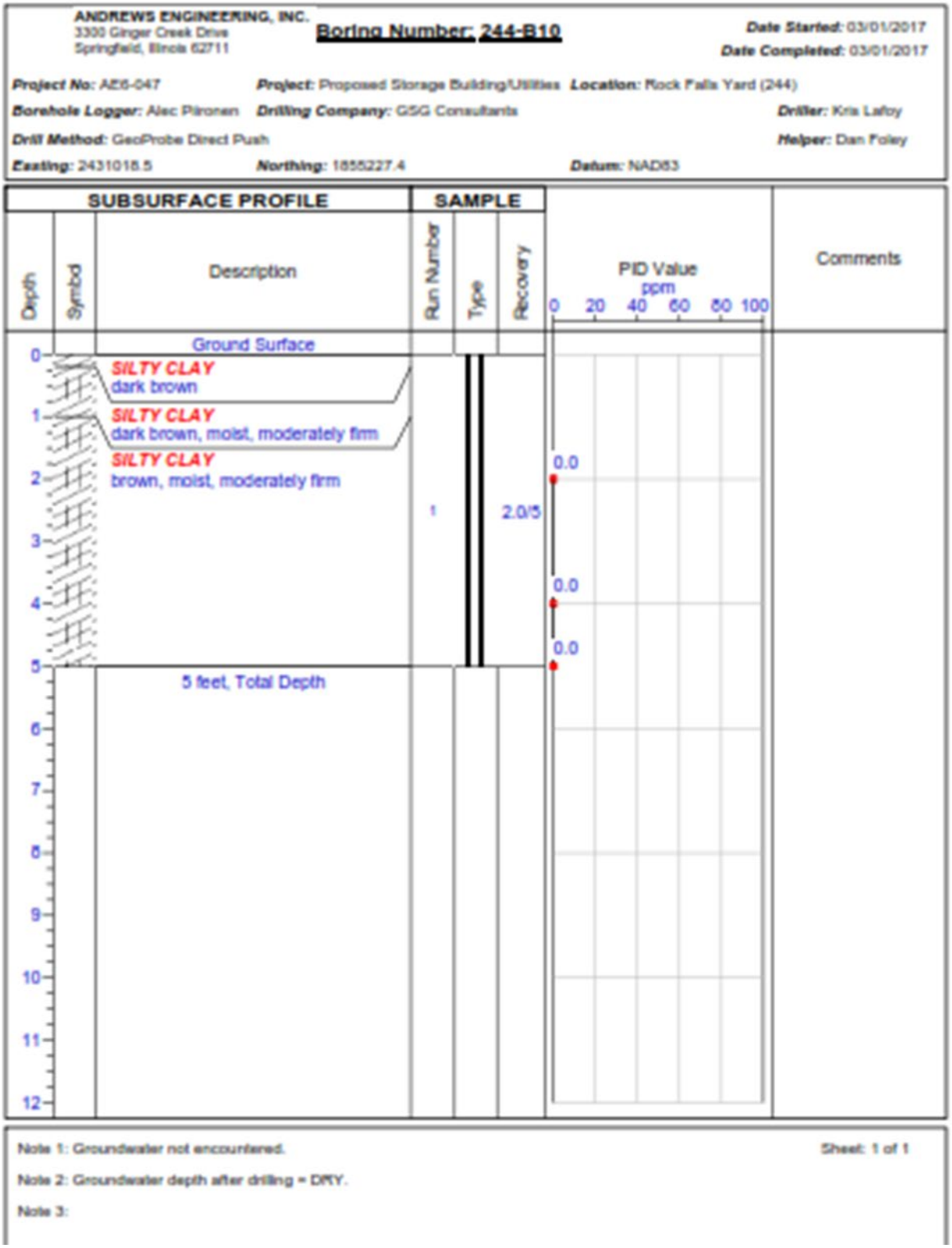

Figure 28. Photo. Soil profile with depth at boring location.

APPENDIX B: LABORATORY TEST DATA

Table 5. Particle Size Distribution

		R1	R2	R3
	Particle Size (x)	Percentage Finer (y)	Percentage Finer (y)	Percentage Finer (y)
SIEVE ANALYSIS				
	9.50	100	100	100
	4.750	98.422	96.584	98.504
	2.000	97.216	93.528	96.208
	0.850	96.080	91.832	94.572
	0.425	87.384	85.036	87.356
	0.250	64.628	68.060	69.160
	0.150	58.692	63.744	64.384
	0.075	57.196	63.568	63.328
HYDROMETER ANALYSIS	0.075	57.196	63.570	63.330
	0.056	52.629	64.848	59.536
	0.040	49.197	63.576	58.269
	0.029	45.192	58.490	53.202
	0.021	37.756	52.132	46.869
	0.015	30.891	45.775	40.535
	0.012	21.738	38.146	36.735
	0.008	18.306	33.060	30.401
	0.006	16.018	30.517	27.868
	0.004	14.873	27.974	25.968
	0.003	12.585	26.066	22.801
	0.001	10.297	21.616	20.268
	%Gravel	2.78	6.47	1.50
	%Sand	42.80	36.40	36.70
	%Silt	44.61	37.50	40.53
	%Clay	12.59	26.07	22.80

Table 6. Atterberg Limit Test for Sample 244-B10 (R1)

	Trial 1		
	Liquid Limit (LL)	Plastic Limit (PL)	Plasticity Index (PI)
Field Soil	22	13	9
Layer 1	20	15	5
Layer 2	27	15	11
Layer 3	29	16	13
Layer 4	26	13	13
	Trial 2		
	Liquid Limit (LL)	Plastic Limit (PL)	Plasticity Index (PI)
Field Soil	23	13	10
Layer 1	18	14	4
Layer 2	24	12	12
Layer 3	31	16	15
Layer 4	30	15	15

Table 7. Atterberg Limit Test for Sample 244-B14 (R2)

	Trial 1		
	Liquid Limit (LL)	Plastic Limit (PL)	Plasticity Index (PI)
Field Soil	45	13	32
Layer 1	38	14	24
Layer 2	36	15	21
Layer 3	35	17	18
Layer 4	40	15	25
	Trial 2		
	Liquid Limit (LL)	Plastic Limit (PL)	Plasticity Index (PI)
Field Soil	42	12	30
Layer 1	38	15	23
Layer 2	34	15	19
Layer 3	33	16	17
Layer 4	36	15	21

Table 8. Atterberg Limit Test for Sample 244-B14 (R3)

	Trial 1		
	Liquid Limit (LL)	Plastic Limit (PL)	Plasticity Index (PI)
Field Soil	24	13	11
Layer 1	46	16	30
Layer 2	42	17	25
Layer 3	40	16	24
Layer 4	40	16	24
	Trial 2		
	Liquid Limit (LL)	Plastic Limit (PL)	Plasticity Index (PI)
Field Soil	25	13	12
Layer 1	46	18	28
Layer 2	46	17	29
Layer 3	43	17	26
Layer 4	39	16	23

Table 9. Daily Measurement for First Reactor Experiment

Day	Anode Well		Cathode Well		Overflow		Outflow Vol	Power Supply		Cathode to Anode		Cathode to Aux		Aux to Anode	
	pH	**Temp.**	**pH**	**Temp.**	**pH**	**Temp.**	**mL**	**Volts**	**Amps**	**Volts**	**Amps**	**Volts**	**Amps**	**Volts**	**Amps**
0	4.34	9.3	4.34	9.3	0	0	0	30	0.15	30	0.149	30	0.476	30	0.454
1	1.23	25.5	13.09	23.9	0	0	0	30	0.382	29.97	0.427	30	0.476	30	0.454
2	1.16	32.5	12.99	27.7	13.17	21	280	30	0.964	29.82	1.052	29.67	1.43	29.91	1.204
3	0.87	33.5	12.97	29.1	13.07	22.1	910	30	1.11	29.62	1.23	29.39	1.74	29.56	1.35
4	nan	nan	12.9	24.8	13	21.2	570	30	0.621	29.9	0.687	29.77	1.176	29.72	0.649
5	nan	nan	12.86	26.8	11.95	21.7	300	30	0.621	29.7	0.69	29.82	1.29	29.67	0.835
6	nan	nan	12.95	25.1	6.22	24	3000	30	0.537	29.88	0.591	29.6	0.968	29.53	0.657
7	3.42	28.2	12.55	27.2	6.01	23.2	3120	30	0.565	29.89	0.605	29.45	0.904	29.82	0.771
8	5.96	25.5	12.73	24.5	7.69	21.1	2360	30	0.406	29.82	0.46	29.88	0.681	29.8	0.532
9	7.49	23.9	11.72	23.4	9.13	20.9	2800	30	0.343	29.84	0.358	29.92	0.468	29.76	0.447
10	6.8	24.4	9.59	25.4	8.25	22.5	2260	30	0.343	29.42	0.289	29.2	0.368	29.95	0.393
11	6	23.2	11.48	22.8	9.01	21.1	20	30	0.26	29.93	0.302	29.86	0.387	29.75	0.408
12	6.65	24.8	12.55	23.5	9.11	23	5	30	0.26	29.73	0.402	29.62	0.468	29.57	0.418
13	4.78	26	5.27	26.4	5.51	22.3	1040	30	0.343	29.91	0.443	29.92	0.6	29.83	0.675
14	3.35	26.9	7.84	27	5.56	22.4	1400	30	0.42	29.89	0.46	29.8	0.667	29.71	0.628

nan: not a number, Aux: Auxiliary, Vol: Volume.

Table 9. Daily Measurement for First Reactor Experiment (Continued)

Day	Anode Well		Cathode Well		Overflow		Outflow Vol	Power Supply		Cathode to Anode		Cathode to Aux		Aux to Anode	
	pH	**Temp.**	**pH**	**Temp.**	**pH**	**Temp.**	**mL**	**Volts**	**Amps**	**Volts**	**Amps**	**Volts**	**Amps**	**Volts**	**Amps**
15	3.88	28.7	7.59	28.8	6.12	23.1	370	30	0.964	29.82	1.052	29.67	1.43	29.91	1.204
16	3.81	26.9	5.73	28.5	4.99	22.3	2100	30	0.509	29.76	2.552	29.83	0.881	29.9	0.764
17	4.42	28.7	5.03	27.9	4.91	21.6	1780	30	0.634	29.9	0.633	29.65	0.952	29.75	0.883
18	4.5	27.7	5.03	27.3	5.15	20.6	2790	30	0.577	29.89	0.614	29.86	0.9	29.51	0.854
19	4.01	27.9	12.73	26.2	7.22	21.8	100	30	0.596	29.93	0.66	29.49	1.35	29.65	0.633
20	6.14	25.5	12.69	25.3	6.98	22.3	5	30	0.561	29.8	0.626	29.59	1.142	29.87	0.739
21	4.58	27.6	5.78	27.1	6.95	26.1	2300	30	0.608	29.79	0.644	29.61	0.992	29.86	0.891
22	3.88	28.7	7.59	28.8	6.12	23.1	370	30	0.964	29.82	1.052	29.67	1.43	29.91	1.204
23	3.86	27.1	5.59	26.5	4.62	21.2	2980	30	0.551	30	0.599	29.87	1.017	29.82	0.754
24	3.59	27.3	3.98	27.8	4.25	22	2400	30	0.553	29.99	0.598	29.69	0.945	29.58	0.757
25	4.32	28.9	4.69	28.7	4.93	22.2	2900	30	0.728	29.92	0.769	29.85	1.273	29.76	0.992
26	4.4	21.7	4.66	21.6	5.12	21.2	2800	30	0.715	29.95	0.763	29.88	1.254	29.74	0.964
27	4.32	28.2	5.02	28.2	5.19	21.8	3000	30	0.78	29.89	0.826	29.83	1.353	29.81	1.043
28	4.36	27.8	4.62	29	4.72	22.2	3470	30	0.704	29.8	0.78	29.55	1.29	29.53	0.964

nan: not a number, Aux: Auxiliary, Vol: Volume.

Table 10. Daily Measurement for Second Reactor Experiment

Day	Anode Well		Cathode Well		Overflow		Outflow Vol	Power Supply		Cathode to Anode		Cathode to Aux		Aux to Anode	
	pH	**Temp.**	**pH**	**Temp.**	**pH**	**Temp.**	**mL**	**Volts**	**Amps**	**Volts**	**Amps**	**Volts**	**Amps**	**Volts**	**Amps**
0	6.14	6.00	6.14	6.00	nan	nan	nan	30	0.74	nan	nan	nan	nan	nan	nan
1	nan	nan	13.30	21.40	13.07	21.40	360	30	0.74	30.00	nan	29.84	2.06	30.00	nan
2	5.79	21.80	12.99	21.30	12.77	20.90	1420	30	0.74	30.00	1.03	29.85	1.53	29.91	1.00
3	1.28	33.00	12.66	28.00	12.66	22.10	942.5	30	1.50	29.59	1.52	29.79	1.90	29.59	1.86
4	0.78	318.00	12.69	31.50	12.95	21.80	1260	30	1.71	29.85	1.56	29.85	1.56	29.81	1.80
5	0.84	29.30	12.81	27.90	13.00	20.70	780	30	1.34	29.83	1.39	29.92	1.34	29.75	1.67
6	nan	nan	12.88	27.20	12.89	22.30	600	30	0.78	29.83	0.68	29.66	1.03	29.83	0.85
7	1.17	27.50	12.56	27.00	12.83	21.50	860	30	0.97	29.70	1.04	29.68	1.12	29.62	1.35
8	3.06	21.20	12.97	24.50	12.28	20.20	1000	30	0.62	29.10	0.67	29.56	1.09	29.06	0.86
9	1.66	33.1	12.77	24.9	10.16	21.7	1260	30	0.657	29.77	0.707	29.67	1.217	29.78	0.86
10	1.53	29.6	12.6	27.1	12.2	22.8	930	30	0.865	29.12	0.933	29.33	1.224	29.35	0.925
11	1.66	28.3	12.79	25.2	12.88	21.4	610	30	0.708	29.48	0.757	29.46	1.065	29.4	0.723
12	1.71	30.2	12.65	24.8	11.81	21.8	1200	30	0.539	29.63	0.613	29.59	0.985	29.04	0.625
13	3.26	25.3	12.35	26.6	6.22	21.5	540	30	0.653	29.46	0.702	29.3	0.973	29.3	0.962
14	3.01	26.6	12.47	27.2	11.79	21.3	650	30	0.762	29.44	0.821	29.1	1.22	29.31	1.073
15	1.7	29.7	12.78	25.6	7.09	21.3	1330	30	0.781	29.32	0.8	29.34	1.322	29.64	0.852
16	4.84	26.8	12.87	25.9	5.23	21.4	1400	30	0.68	29.54	0.761	29.53	1.039	29.78	0.998
17	2.04	27.6	12.8	23.7	12.59	19.5	1170	30	0.661	29.83	0.7	29.8	1.017	29.65	0.768

nan: not a number, Aux: Auxiliary, Vol: Volume.

Table 11. Daily Measurement for Third Reactor Experiment

Day	Anode Well		Cathode Well		Overflow		Overflow Vol	Power Supply		Cathode to Anode		Cathode to Aux		Aux to Anode	
	pH	**Temp.**	**pH**	**Temp.**	**pH**	**Temp.**	**mL**	**Volts**	**Amps**	**Volts**	**Amps**	**Volts**	**Amps**	**Volts**	**Amps**
0	4.5	nan	4.5	nan	4.5	nan	0	30	0.894	nan	nan	nan	nan	nan	nan
1	1.32	37.6	13.1	29.4	13.11	21.4	100	30	1.76	29.23	1.921	29.33	2.198	29.4	1.592
2	1.48	35.6	12.98	24.9	13.03	19.9	160	30	1.47	29.62	1.435	29.3	2.434	29.35	1.409
3	2.04	28.2	13.02	22.4	12.83	19.1	490	30	0.764	29.77	0.833	29.47	2.212	29.58	0.922
4	1.91	29.6	12.91	22.5	12.57	20.5	700	30	0.714	29.66	0.731	29.33	1.9	29.64	0.736
5	1.7	26.9	12.73	20.3	12.55	18.6	430	30	0.724	29.67	0.785	29.19	2.854	29.71	0.84
6	1.23	28.1	12.64	20.9	12.64	18.2	260	30	0.692	29.78	0.75	29.49	2.451	29.75	0.75
7	1.69	27.9	12.69	21.6	12.53	19.8	250	30	0.822	29.96	0.854	29.76	1.932	29.87	0.84
8	1.76	25.3	12.78	20	12.72	17.5	530	30	0.681	29.9	0.73	29.8	1.76	29.76	0.73
9	2.1	29.4	12.9	24.6	12.88	12.9	630	30	0.761	29.93	0.801	29.46	1.731	29.79	0.836
10	2.03	30	12.45	26.1	12.61	21.8	330	30	0.663	29.67	0.723	29.61	1.433	29.7	0.884
11	2.18	33.5	12.92	25.3	12.53	23.6	290	30	0.736	29.74	0.794	29.37	2.091	29.61	0.848
12	2.64	30	13.04	25.8	12.87	24.7	280	30	0.564	29.89	0.698	29.63	2.104	29.87	0.756
13	1.86	32.5	12.88	26.3	12.73	24.1	340	30	0.663	29.87	0.703	29.51	1.651	29.79	0.792
14	1.94	31.4	12.86	25.9	12.61	24.5	250	30	0.579	29.78	0.632	29.76	1.403	29.82	0.735

nan: not a number, Aux: Auxiliary, Vol: Volume.


Illinois Department
of Transportation


ILLINOIS